Role of transglutaminase 2 in PAC_1 receptor mediated protection against hypoxia-induced cell death and neurite outgrowth in differentiating N2a neuroblastoma cells

Alanood S. ALGARNI, Alan J. HARGREAVES, John M. DICKENSON*

School of Science and Technology

Nottingham Trent University

Clifton Lane

Nottingham

NG11 8NS

*To whom correspondence should be addressed

Tel: +44-1158486683

E-mail: john.dickenson@ntu.ac.uk

Running title: Activation of TG2 by the PAC_1 receptor

Abbreviations used: BSA, bovine serum albumin; DAG, diacylglycerol; DMEM, Dulbecco's modified Eagle's medium; ERK1/2, extracellular signal-regulated kinases 1 and 2; FITC, fluorescein isothiocyanate; GPCRs, G-protein coupled receptors; HRP, horseradish peroxidase; JNK, c-Jun N-terminal kinase; LDH, lactate dehydrogenase; MAPK, mitogen activated protein kinase; MEK1/2, mitogen-activated protein kinase kinase 1/2; PACAP, pituitary adenylate cyclase-activating polypeptide; PBS, phosphate-buffered saline; PKA, protein kinase A; PKB, protein kinase B; PKC, protein kinase C; SDS-PAGE, sodium dodecyl sulphate polyacrylamide gel electrophoresis;

Abstract

The PAC_1 receptor and tissue transglutaminase (TG2) play important roles in neurite outgrowth and modulation of neuronal cell survival. In this study, we investigated the regulation of TG2 activity by the PAC_1 receptor in retinoic acid-induced differentiating N2a neuroblastoma cells. TG2 transamidase activity was determined using an amine incorporation and a peptide cross linking assay. In situ TG2 activity was assessed by visualising the incorporation of biotin-X-cadaverine using confocal microscopy. TG2 phosphorylation was monitored via immunoprecipitation and Western blotting. The role of TG2 in PAC_1 receptor-induced cytoprotection and neurite outgrowth was investigated by monitoring hypoxia-induced cell death and appearance of axonal-like processes, respectively. The amine incorporation and protein crosslinking activity of TG2 increased in a time and concentration-dependent manner following stimulation with pituitary adenylate cyclase-activating polypeptide-27 (PACAP-27). PACAP-27 mediated increases in TG2 activity were abolished by the TG2 inhibitors Z-DON and R283 and by pharmacological inhibition of protein kinase A (KT 5720 and *Rp*-cAMPs), protein kinase C (Ro 31-8220), MEK1/2 (PD 98059), and removal of extracellular Ca^{2+}. Fluorescence microscopy demonstrated PACAP-27 induced *in situ* TG2 activity. TG2 inhibition blocked PACAP-27 induced attenuation of hypoxia-induced cell death and outgrowth of axon-like processes. TG2 activation and cytoprotection were also observed in human SH-SY5Y cells. Together, these results demonstrate that TG2 activity was stimulated downstream of the PAC_1 receptor via a multi protein kinase dependent pathway. Furthermore, PAC_1 receptor-induced cytoprotection and neurite outgrowth are dependent upon TG2. These results highlight the importance of TG2 in the cellular functions of the PAC_1 receptor.

Keywords: PACAP, PAC_1 receptor, transglutaminase 2, neuroblastoma cells, cytoprotection, neurite outgrowth

1. Introduction

Transglutaminases (TGs) are a family of Ca^{2+})-dependent enzymes that catalyse the post-translational modification of proteins (for extensive reviews see Nurminskaya and Belkin, 2012; Eckert *et al*., 2014). There are eight distinct catalytically active members of the TG family which exhibit differential expression (Factor XIIIa and TGs 1-7).

The ubiquitously expressed TG2 is the most widely studied member of the TG family which is involved in the regulation of numerous cellular processes, including cell adhesion, migration, growth, survival, apoptosis, differentiation, and extracellular matrix organization (Nurminskaya and Belkin, 2012). In neuronal cells, TG2 is involved in neural differentiation, neurite outgrowth and neuroprotection following cerebral ischaemia (Tucholski *et al*., 2001; Filiano *et al*., 2010; Vanella *et al*., 2015).

Transglutaminase 2 (TG2) possesses multiple enzymic functions that include transamidation, protein disulphide isomerase and protein kinase activity (Gundemir *et al.,* 2012). The transamidase activity of TG2 is inhibited by GTP/GDP and evidence suggests that TG2 when bound to GTP/GDP functions as a G-protein (known as Gh; Mhaouty-Koja, 2004), which is independent of its transamidase activity. Indeed, several members of the G-protein coupled receptor (GPCR) family including the α_{1B}-adrenergic receptor, thromboxane A2 receptor and oxytocin receptor couple to Gh when activated, promoting exchange of GDP for GTP (Gundemir *et al*., 2012). Activated Gh-GTP stimulates phospholipase C δ1 promoting phosphoinositide hydrolysis and stimulating increases in intracellular Ca^{2+}.

The activity of TG2 and other TG family members can be regulated by protein kinases. For example, phosphorylation of TG2 by protein kinase A (PKA) inhibits its transamidating activity but enhances its kinase activity (Mishra *et al.,* 2007). The transamidating activity of TG1 (keratinocyte transglutaminase) is enhanced by phorbol ester-induced stimulation of protein kinase C (PKC) and extracellular signal-regulated kinase 1/2 (ERK1/2; Bollag *et al.,* 2005). These findings suggest that the activity of TG can be regulated by signaling pathways associated with GPCRs. However, the regulation of intracellular TG2 following stimulation of GPCRs is not well understood. Examples include muscarinic receptor-mediated increases in TG2 activity in SH-SY5Y cells (Zhang *et al*., 1998), 5-HT_{2A} receptor-mediated transamidation of Rac1 in the rat A1A1v cortical cell line (Dai *et al*., 2008) and A_1 adenosine receptor-mediated increases in TG2 transamidase activity in rat H9c2 cardiomyoblasts (Vyas *et al*., 2016).

Of particular interest to the current study is pituitary adenylate cyclase-activating polypeptide (PACAP), which is widely distributed in the brain and peripheral organs and

displays high affinity for the PAC_1 receptor (Vaudry et al., 2009). The PAC_1 receptor is a member of the GPCR superfamily which activates adenylyl cyclase/cAMP/PKA (via G_s-protein coupling) and phospholipase C/DAG/PKC (via G_q-protein coupling) dependent signalling pathways (Dickson and Finlayson, 2009; Vaudry et al., 2009). The PAC_1 receptor also triggers the activation of several other protein kinase cascades such as ERK1/2, JNK1/2, p38 MAPK and PKB (Monaghan *et al*., 2008; May *et al*., 2010, Castorina *et al*. 2014). Since some of these protein kinase pathways are associated with modulation of TG activity (PKA, PKC and ERK1/2) it is conceivable that the PAC_1 receptor regulates TG activity. Since mouse N2a neuroblastoma cells express PAC_1 receptors (Leliévre et al., 1998; Miura et al., 2013;) the primary aims of this study were (i) to determine whether the PAC_1 receptor modulates TG2 activity in these cells and (ii) to assess the role of TG2 in PAC_1 receptor-induced neuroprotection and neurite outgrowth The results obtained indicate that PAC_1 receptor stimulation triggers TG2-mediated amine incorporation and protein cross-linking activity in differentiating N2a and SH-SY5Y cells. Furthermore, inhibition of TG2 attenuates PAC_1 receptor-induced cytoprotection and neurite outgrowth.

2. Materials and Methods

2.1. *Materials*

Akt inhibitor XI, KT 5720, Ro-31-8220 and *R*p-8-Cl-cAMPS (adenosine 3',5'-cyclic monophosphorothioate, 8-chlro-, Rp-isomer) were purchased from Calbiochem (San Diego, CA). [Ala^{11,22,28}]-VIP, Bay 55-9837, PACAP-27, PACAP 6-38, PD 98059, SB 203580, and SP 600 125 were obtained from Tocris Bioscience (Bristol, UK). *All-trans* retinoic acid, casein, Protease Inhibitor Cocktail (for use with mammalian cell and tissue extracts), Phosphatase Inhibitor Cocktail 2 and 3, ExtrAvidin®-HRP and ExtrAvidin®-FITC were obtained from Sigma-Aldrich Co. Ltd. (Gillingham, UK). The TG2 inhibitors Z-DON (Z-ZON-Val-Pro-Leu-OMe) and R283, together with purified guinea-pig liver TG2 were obtained from Zedira GmbH (Darmstadt, Germany). DAPI was from Vector Laboratories Inc (Peterborough, UK). Fluo-8/AM was purchased from Stratech Scientific Ltd (Newmarket, UK). Biotin-TVQQEL was purchased from Pepceuticals (Enderby, UK). Biotin cadaverine (N-(5-aminopentyl)biotinamide) and biotin-X-cadaverine (5-([(N-(biotinoyl)amino)hexanoyl]amino)pentylamine) were purchased from Invitrogen, UK. Dulbecco's modified Eagle's medium (DMEM), foetal bovine serum, trypsin (10×), L-glutamine (200 mM), penicillin (10,000 U/ml)/streptomycin (10,000 μg/ml) were purchased from BioWhittaker Ltd, UK. All other reagents were purchased from Sigma-Aldrich Co. Ltd. (Gillingham, UK) and were of analytical grade.

Antibodies were obtained from the following suppliers: monoclonal anti-phospho ERK1/2 (Thr^{202}/Tyr^{204}) and polyclonal anti-tyrosine hydroxylase from Sigma-Aldrich; polyclonal anti-phospho PKB (Ser^{473}), polyclonal anti-total PKB, monoclonal anti-total ERK1/2, monoclonal anti-phospho p38 MAPK, polyclonal anti-total p38 MAPK, monoclonal anti-phospho JNK1/2, polyclonal anti-total JNK1/2 and polyclonal anti-cleaved caspase 3 from New England Biolabs Ltd (UK); polyclonal anti-human keratinocyte TG1 and polyclonal anti-human epidermal TG3 from Zedira GmbH (Darmstadt, Germany); monoclonal anti-TG2 (CUB 7402) from Thermo Scientific (Leicestershire, UK); monoclonal anti-GAPDH, polyclonal anti-phosphoserine and polyclonal anti-phosphothreonine from Abcam (Cambridge, UK); polyclonal anti-choline acetyltransferase from Santa Cruz Biotechnology Inc (Heidelberg, Germany).

2.2. *Cell Culture*

Murine N2a and human SH-SY5Y neuroblastoma cells were obtained from the European Collection of Animal Cell Cultures (Porton Down, Salisbury, UK). Cells were cultured in DMEM supplemented with 2 mM L-glutamine, 10% (v/v) foetal bovine serum, penicillin (100 U/ml) and streptomycin (100 μg/ml). Cells were maintained in a humidified incubator (95% air/5% CO_2 at 37°C) until 70-80% confluent and sub-cultured (1:5 split ratio) every 3-4 days. SH-SY5Y cells were sub-cultured using trypsin (0.05% w/v)/EDTA (0.02% w/v).

Differentiation of N2a cells was induced by culturing cells in serum-free DMEM containing 1 μM *all-trans* retinoic acid for 48 h, unless otherwise specified. Differentiation of SH-SY5Y cells was induced by culturing cells in serum-free DMEM containing 10 μM *all-trans* retinoic acid for 5 days. Experiments were performed on passage numbers 8-20 for N2a and 18-25 for SH-SY5Y.

2.3. *cAMP accumulation assay*

N2a cells (5000 cells $well^{-1}$) were seeded on a white 96 well microtitre plate, with clear bottomed wells (Corning; Fisher Scientific, Loughborough, UK) and induced to differentiate as described above. The medium was then removed and the monolayer treated with a range of concentrations of PACAP-27 for 20 min in serum-free DMEM (40 μl $well^{-1}$) in the presence of 20 mM $MgCl_2$ and 500 μM 3-isobutyl-1-methylxanthine (IBMX). Following stimulation, cAMP levels within cells were determined using the cAMP-Glo™ Max Assay kit (Promega; Southampton, UK). Briefly, 10 μl of cAMP detection solution was added to all wells and incubated for 20 min at room temperature. After incubation, Kinase-Glo® reagent (50 μl $well^{-1}$) was added and incubated for 10 min at room temperature, following which luminescence levels across the plate were recorded using a plate-reading FLUOstar Optima luminometer (BMG Labtech Ltd, UK,). Treatment with forskolin (10 μM) was used as a positive control and the luminescence values were converted to cAMP levels using a cAMP standard curve (0-100 nM), according to the manufacturer's instructions.

2.4. *Cell extraction for measurement of TG2 activity*

Time course profiles and concentration-response curves were obtained for PACAP-27. Where appropriate, cells were also pre-incubated for 30 min in medium with or without the protein kinase inhibitors *Rp*-cAMPs (PKA, 50 μM; de Wit et al., 1984), KT 5720 (PKA, 5 μM; Kase et al., 1987), Akt inhibitor XI (PKB/Akt, 100 nM; Barve et al., 2006), PD 98059 (MEK1/2, 50 μM; Dudley et al., 1995), SP 600125 (JNK1/2, 20 μM; Bennett et al., 2001), and Ro 31-8220 (PKC, 10 μM; Davies et al., 1989) prior to treatment with 100 nM PACAP-27. The concentrations of protein kinase inhibitors employed in this study were in the range of values in the literature that are used to inhibit the cellular activity of these kinases: KT 5720 (2-10 μM; Werner et al., 2014; Mangiavacchi and Wolf, 2004); *Rp*-cAMPs (10-100 μM; Werner et al., 2014; Mangiavacchi and Wolf, 2004; Wang et al., 2012; Pratt et al., 2016; Vallejo and Vallejo, 2002); Ro 31-8220 (1-10 μM; Lee et al., 2013; Montejo-López et al., 2016), PD 98059 (10-50 μM; Sutter et al., 2004; Kim et al., 2008), SP 600125 (20 μM; Hah et al., 2013; Kim et al., 2010) and Akt inhibitor XI (1 μM; Frampton et al.,2012; Rybchyn et al., 2011). In the case of less well known Akt inhibitor XI effects on PKB inhibition were verified by Western blot analysis.

Following stimulation, N2a and SH-SY5Y cells were rinsed twice with 2.0 ml of chilled PBS, lysed with 500 µl of ice-cold lysis buffer (50 mM Tris-HCl pH 8.0, 0.5% (w/v) sodium deoxycholate, 0.1% (v/v) Protease Inhibitor Cocktail, and 1% (v/v) Phosphatase Inhibitor Cocktail 2). Cell lysates were scraped and clarified by centrifugation at 4°C for 10 min at 14000 x g prior to being assayed for TG activity using the biotin-labeled cadaverine incorporation assay (see below). Supernatants were collected and stored at -80°C.

Protein levels were determined by the bicinchoninic acid (BCA) protein assay, based on the method of Smith et al. (1985), which was performed using a commercially available kit (Sigma-Aldrich, UK) using bovine serum albumin (BSA) as the standard. Transglutaminase activity was monitored by two different transamidase assays; amine incorporation and protein cross-linking.

2.5. *Biotin-labeled cadaverine incorporation assay*

The assay was performed as per the method described by Slaughter et al. (1992) with the modifications of Lilley et al. (1998). Briefly, 96-well microtitre plates were coated overnight at 4°C with 250 µl of N',N'-dimethylcasein (10 mg ml^{-1} in 100 mM Tris-HCl, pH 8.0). The plate was washed twice with distilled water and blocked with 250 µl of 3% (w/v) BSA in 100 mM Tris-HCl, pH 8.0 and incubated for 1 h at room temperature. The plate was washed twice before the application of 150 µl of either 6.67 mM calcium chloride and or 13.3 mM EDTA (used to deplete calcium and suppress TG activity) assay buffer containing 225 µM biotin cadaverine (a widely used substrate to monitor TG amine incorporating activity) and 2 mM 2-mercaptoethanol. The reaction was started by the addition of 50 µl of samples or positive control (50 ng/well of guinea-pig liver TG2) and negative control (100 mM Tris-HCl, pH 8.0). After incubation for 1 h at 37°C plates were washed as before. Then, 200 µl of 100 mM Tris-HCl pH 8.0 containing 1% (w/v) BSA and ExtrAvidin®-HRP (1:5000 dilution) was added to each well and the plate incubated at 37°C for 45 min then washed as before. The plate was developed with 200 µl of freshly made developing buffer (7.5 µg ml^{-1} 3,3',5,5'-tetramethylbenzidine (TMB) and 0.0005% (v/v) H_2O_2 in 100 mM sodium acetate, pH 6.0) and incubated at room temperature for 15 min. The reaction was terminated by adding 50 µl of 5 M sulphuric acid and the absorbance read at 450 nm. One unit of TG2 was defined as a change in absorbance of one unit h^{-1}. Each experiment was performed in triplicate.

2.6. *Biotin-labeled peptide-cross-linking assay*

The assay was performed according to the method of Trigwell et al. (2004) with minor modifications. Microtitre plates (96-well) were coated and incubated overnight at 4°C with casein at 1.0 mg ml^{-1} in 100 mM Tris-HCl pH 8.0 (250 µl per well). The wells were

washed twice with distilled water, before incubation at room temperature for 1 h with 250 µl of blocking solution (100 mM Tris-HCl pH 8.0 containing 3% (w/v) BSA). The plate was washed twice before the application of 150 µl of either 6.67 mM calcium chloride and or 13.3 mM EDTA assay buffer containing 5 µM biotin-TVQQEL and 2mM 2-mercaptoethanol. The reaction was started by the addition of 50 µl of samples or positive control (50 ng/well of guinea-pig liver TG2) and negative control (100 mM Tris-HCl, pH 8.0) and allowed to proceed for 1 h at 37°C. Reaction development and termination were performed as described for biotin-cadaverine assays. One unit of TG2 was defined as a change in absorbance of one unit h^{-1}. Each experiment was performed in triplicate.

2.7. *Hypoxia-induced cell death*

Differentiating N2a and SH-SY5Y cells in glucose-free and serum-free DMEM (Gibco™, Life Technologies Ltd, Paisley, UK) were exposed to hypoxia using a hypoxic incubator (5% CO_2/1% O_2 at 37°C) in which O_2 was replaced by N_2.

2.8. *Cell viability assays*

N2a and SH-SY5Y cells were plated in 24-well flat bottomed plates (15,000 cells/well) and differentiated for 48 h, before cell viability was determined by measuring the reduction of MTT (Mosmann et al., 1983). The amount of DMSO-solubilised reduced formazan product was determined by measurement of absorbance at a wavelength 570 nm. Alternatively, cells were plated in 96-well flat bottomed plates (5,000 cells per well) and differentiated for 48 h. Following normoxia/hypoxia exposure, the activity of lactate dehydrogenase (LDH) released into the culture medium was detected using the CytoTox 96®non-radioactive cytotoxicity assay (Promega, Southampton, UK) with measurement of absorbance at 490 nm.

2.9. *Outgrowth of axon-like processes*

The outgrowth of axon-like processes in N2a cells was assessed as described previously (Hargreaves *et al*., 2006). N2a cells were seeded in 24-well plates (25,000 cells/well) and incubated for 24 h in growth medium prior to treatment with PACAP-27 (100 nM) in serum-free DMEM for 24 or 48 h. After stimulation, the cells were washed with ice cold phosphate buffered saline (PBS) then fixed in 90% (v/v) methanol in PBS at -20°C for 15 min. After washing, the cells were stained for 1 min at room temperature with Coomassie brilliant blue, washed with PBS then with distilled water. The outgrowth of axon-like processes was morphologically assessed using an inverted light microscope. Five randomly selected fields, containing at least 200 cells, were examined in each well. The total number of cells and the number of axon-like processes, defined as extensions

greater than two cell body diameters in length with an extension foot (Keilbaugh *et al*., 1991) were recorded.

2.10. *Western blot analysis*

Protein extracts (15-20 µg per lane) were separated by SDS-PAGE (10% w/v polyacrylamide gel) using a Bio-Rad Mini-Protean III system. Proteins were transferred to nitrocellulose membranes in a Bio-Rad Trans-Blot system using 25 mM Tris, 192 mM glycine pH 8.3 and 20% (v/v) MeOH). Following transfer, the membranes were washed with Tris-buffered saline (TBS) and blocked for 1 h at room temperature with 3% (w/v) skimmed milk powder in TBS containing 0.1% (v/v) Tween-20. Blots were then incubated overnight at 4^{o}C in blocking buffer with primary antibodies to the following targets (1:1000 dilutions unless otherwise indicated): phospho-specific ERK1/2, phospho-specific PKB (1:500), phospho-specific p38 MAPK, phospho-specific JNK (1:500), cleaved active caspase-3 (1:500), GAPDH, TG1, TG2 or TG3. The primary antibodies were removed and blots washed three times for 5 min in TBS/Tween 20. Blots were then incubated for 2 h at room temperature with the appropriate secondary antibody (1:1000) coupled to horseradish peroxidase (New England Biolabs Ltd; UK) in blocking buffer. Following removal of the secondary antibody, blots were extensively washed as above and developed using the Enhanced Chemiluminescence Detection System (Uptima, Interchim, France) and quantified by densitometry using Advanced Image Data Analysis Software (Fuji; version 3.52). The uniform transfer of proteins to the nitrocellulose membrane was routinely monitored by transiently staining the membranes with Ponceau S stain prior to application of the primary antibody. When assessing protein kinase phosphorylation samples from each experiment were also analysed on separate blots using primary antibodies that recognise total ERK1/2, PKB, p38 MAPK and JNK1/2 (all 1:1000 dilution) in order to confirm the uniformity of protein loading.

2.11. *Visualisation of in situ TG2 activity and neuronal markers*

N2a cells were seeded on 8-well chamber slides (15,000 cells well^{-1}) and differentiated for 48 h in serum-free DMEM containing retinoic acid or PACAP-27 (100 nM). The medium was then removed, monolayer gently washed with PBS and slides incubated for 6 h with 1 mM biotin-X-cadaverine (a cell permeable TG2 substrate; Perry et al., 1995) in serum-free DMEM experimentation. Where appropriate, cells were treated for 1 h with TG2 inhibitors Z-DON (150 µM) or R283 (200 µM) before the addition of 100 nM PACAP-27. Following stimulation, cells were fixed with 3.7 % (w/v) paraformaldehyde and permeabilised with 0.1% (v/v) Triton-X100 both in PBS for 15 min at room temperature. After washing, cells were blocked with 3% (w/v) BSA for 1 h at room temperature and the transglutaminase mediated biotin-X-cadaverine labeled protein substrates detected

by (1:200 v/v) FITC-conjugated ExtrAvidin® (Sigma-Aldrich). For the visualisation of neuronal markers fixed cell monolayers were incubated overnight at 4°C with rabbit anti-choline acetyltransferase antibody (1:200) or mouse anti-tyrosine hydroxylase antibody (1:200) in 3% (w/v) BSA. Unbound primary antibody was then removed, and the cells washed three times for 5 min with PBS. Cells were then incubated for 2 h at 37°C in a humidified chamber with either goat anti-mouse or anti-rabbit FITC-conjugated immunoglobulin G (Abcam, Cambridge, UK) diluted 1:1000 in 3% (w/v) BSA. The chamber slide was subsequently washed three times for 5 min with PBS, air-dried and mounted with Vectashield® medium (Vector Laboratories Ltd, Peterborough, UK) containing DAPI counterstain for nuclei visualisation. Finally slides were sealed using clear, colourless nail varnish and stained cells visualised using a Leica TCS SP5 II confocal microscope (Leica Microsystems, GmbH, Manheim, Germany) equipped with a 20x air objective. Optical sections were typically 1-2 µm and the highest fluorescence intensity values were acquired and fluorescence intensity relative to DAPI stain quantified for each field of view. Saturation was avoided using the look-up Table overlay provided by the software. Image analysis and quantification were carried out using Leica LAS AF software.

2.12. *Measurement of intracellular calcium*

N2a cells were plated in 24-well flat-bottomed plates (15,000 cells well^{-1}) and differentiated for 48 h. Cells were loaded with Fluo-8 AM (5 µM, 30-40 min) before mounting on the stage of an Leica TCS SP5 II confocal microscope (Leica Microsystems, GmbH, Manheim, Germany) equipped with a 20x air objective. Cells were incubated at 37°C using a temperature controller and micro incubator (The Cube, Life Imaging Services, Basel, Switzerland) in the presence of imaging buffer (134 mM NaCl 134, 6 mM KCl 6, 1.3 mM $CaCl_2$ 1 mM $MgCl_2$ 1, 10 mM HEPES, and 10 mM glucose; pH 7.4). Using an excitation wavelength of 490 nm , emissions over 514 nm were recorded. Images were collected every 1.7 s for 10 min. Relative increases in intracellular Ca^{2+} were defined as F/F_0 where F was the fluorescence at any given time, and F_0 was the initial basal level of Ca^{2+}.

2.13. *Determination of TG2 phosphorylation*

Following stimulation, differentiated N2a cells were rinsed twice with 2.0 ml of chilled PBS and lysed with 500 µl of ice-cold lysis buffer (2 mM EDTA, 1.5 mM $MgCl_2$, 10% (v/v) glycerol, 0.5% (v/v) IGEPAL, 0.1% (v/v) Protease Inhibitor Ccocktail, and 1% (v/v) Phosphatase Inhibitor Cocktail 2 and 3 in PBS). Cell lysates were clarified by

centrifugation (4°C for 10 min at 14000 x g), after which 500 µg of supernatant protein were incubated overnight at 4°C with 2 µg of anti-TG2 monoclonal antibody or IgG. Immune complexes were precipitated using Pierce™ Classic Magnetic IP/Co-IP Kit (Loughborough, UK). The precipitates were resolved by SDS-PAGE and Western blotting, then probed using anti-phosphoserine or anti-phosphothreonine antibodies (1:1000). Antibody reactivity was visualised by ECL and quantified densitometrically, as described above.

2.14. *Statistical analysis*

All graphs and statistics (one-way ANOVA followed by Dunnet's multiple comparison test and two-way ANOVA for group comparison) were performed using GraphPad Prism® software (GraphPad Software, Inc., USA). Agonist EC_{50} values (concentration of agonist producing 50% of the maximal stimulation) were obtained by computer-assisted curve fitting using GraphPad Prism® software. Agonist $p[EC_{50}]$ values were subsequently calculated as the negative logarithm to base 10 of the EC_{50}. Results represent mean ± S.E.M. and p values <0.05 were considered statistically significant.

3. Results

3.1. *Characterisation of cholinergic neuronal phenotype and TG expression pattern in N2a cells*

Mouse N2a neuroblastoma cells can be differentiated into various neuronal types dependent upon the method used (Manabe *et al*., 2005; Tremblay *et al*., 2010). For example, serum withdrawal in the presence of retinoic acid induces differentiation into cholinergic neurons, whereas dibutyryl cAMP promotes the development of dopaminergic neurons (Manabe *et al*., 2005; Tremblay *et al*., 2010). In this study N2a cells were induced to differentiate using retinoic acid in order to avoid potential problems using dibutyryl cAMP when assessing functional responses mediated by the G_s-protein coupled PAC_1 receptor. Immunocytochemical staining indicated that expression of the cholinergic neuronal marker, choline acetyltransferase increased markedly after 48 h confirming that retinoic acid promotes differentiation of N2a cells into cholinergic neurons (Fig 1A and B).

Western blot analysis was performed to compare the expression of TG isoforms in mitotic and differentiating N2a cells. TG1, TG2 and TG3 expression increased significantly in N2a cells following differentiation for 48 h with 1 μM *all-trans* retinoic acid (Fig. 1C and D). These observations are in agreement with previous studies (Condello *et al*., 2008).

3.2. *Effect of PAC_1 receptor activation on TG2 activity*

PACAP-27 induced a robust increase in cAMP accumulation (EC_{50} = 4.0 ± 1.3 nM; $p[EC]_{50}$ = 8.5 ± 0.2; n=3) in retinoic acid-induced differentiating N2a cells (Fig. 2). The selective $VPAC_1$ and $VPAC_2$ agonists, $[Ala^{11,22,28}]$-VIP (1 μM) and Bay 55-9837 (1 μM) respectively, had no significant effect on cAMP accumulation (data not shown). PACAP-27 treatment produced transient increases in TG2 catalysed biotin-cadaverine incorporation and protein cross-linking activity, peaking at 10 min (Fig. 3A and C). Furthermore, as shown in Fig. 3, PACAP-27 stimulated concentration-dependent increases in biotin-amine incorporation activity (EC_{50} = 0.08 ± 0.01 nM; $p[EC_{50}]$ = 10.1 ± 0.1; n=5) and protein cross-linking activity (EC_{50} = 0.4 ± 0.2 nM; $p[EC_{50}]$ = 9.7 ± 0.2; n=6). The selective PAC_1 receptor antagonist PACAP 6-38 attenuated PACAP-27 induced biotin-amine incorporation activity (Fig. 4A) and protein cross-linking activity (Fig. 4B). The selective $VPAC_1$ and $VPAC_2$ agonists, $[Ala^{11,22,28}]$-VIP (1 μM) and Bay 55-9837 (1 μM) respectively, had no significant effect on TG2 activity (data not shown). Overall, these data indicate that the PAC_1 receptor is functionally expressed and stimulates TG2-mediated transamidase activity in differentiated N2a cells.

3.3. *Effect of TG2 inhibitors on PAC_1 receptor induced TG2 activity*

To confirm that TG2 is responsible for PAC_1 receptor-mediated transglutaminase activity in differentiating N2a cells, two structurally different cell permeable TG2 specific inhibitors were tested; R283 (a small molecule; Freund *et al.,* 1994) and Z-DON (peptide-based; Schaertl *et al.,* 2010). N2a cells were pre-treated for 1 h with Z-DON (150 μM) or R283 (200 μM) prior to stimulation with PACAP-27 for 10 min. Both inhibitors completely blocked PACAP-27-induced TG-mediated amine incorporation (Fig. 4C) and protein cross-linking activity (Fig. 4D). It is important to note that despite these TG2 inhibitors being cell-permeable, inhibition of cellular TG2 is only achieved at concentrations significantly above their IC_{50} value versus purified enzyme (Schaertl *et al*., 2010; Freund *et al.,* 1994). Overall, these data indicate that TG2 is the TG isoform activated by the PAC_1 receptor.

3.4. *The effect of protein kinase inhibitors on PAC_1 receptor-induced TG2 activity*

Pre-treatment with the PKA inhibitors KT 5720 (5 μM) and *Rp*-cAMPs (50 μM) completely abolished PACAP-27-induced amine incorporation (Fig. 4E) and protein cross-linking activity (Fig. 4F), confirming the involvement of PKA in TG2 activation via the PAC_1 receptor.

Modulation of protein kinase activity following PAC_1 receptor activation was assessed by Western blotting using phospho-specific antibodies that recognise phosphorylated motifs within activated ERK1/2 (pTEpY), p38 MAPK (pTGpY), JNK (pTPpY) and PKB (S^{473}). PACAP-27 (100 nM) stimulated significant increases in ERK1/2 (Fig. 5A), PKB (Fig. 5B) and JNK1/2 (Fig. 5C) phosphorylation in differentiating N2a cells. As expected PACAP-27-mediated increases in ERK1/2, PKB and JNK1/2 phosphorylation were inhibited by PD 98059 (50 μM; MEK1/2 inhibitor; Fig. 5A), Akt inhibitor XI (0.1, 1 μM and 10 μM; PKB inhibitor; Fig. 5B) and SP 600125 (20 μM; JNK1/2 inhibitor; Fig. 5B), respectively. No significant increases in p38 MAPK phosphorylation were observed following PACAP-27 (100 nM for 10 min) treatment (data not shown). PACAP-27–induced increases in ERK1/2 were also attenuated by KT 5720 (5 μM; PKA inhibitor; Fig. 6A) and Ro 31-8220 (10 μM; PKC inhibitor; Fig. 6B), but not following removal of extracellular Ca^{2+} (Fig. 6C). In summary, these data have shown that PAC_1 receptor activation in differentiating N2a cells triggers robust increases in ERK1/2, PKB and JNK1/2 phosphorylation and that ERK1/2 activation is PKA and PKC dependent.

The role of ERK1/2, PKB, PKC and JNK1/2 in PAC_1 receptor-induced TG2 activation was determined using pharmacological inhibitors of these protein kinases. PACAP-27-induced transglutaminase-mediated amine incorporation activity and protein cross-linking activity were inhibited by PD 98950, Ro 318220, and Akt inhibitor XI, suggesting the involvement

of ERK1/2, PKC and PKB, respectively, in PAC_1 receptor-mediated TG2 responses (Fig. 7 A-D). In contrast, SP 6000125 attenuated PACAP-27-induced protein cross-linking activity (Fig. 7F) but was without effect on TG2-mediated amine incorporation (Fig. 7E). Finally, PD 98059, Ro 31-8220, Akt inhibitor XI, and SP 600125 had no significant effect on purified guinea pig liver TG2 activity (data not shown). Overall, these data suggest that the PAC_1 receptor stimulates TG2 activity in differentiating N2a cells via a multi protein kinase dependent pathway.

3.5. *Visualisation of in situ TG2 activity following PACAP treatment*

Biotin-X-cadaverine, is a cell penetrating primary amine, which enables the *in situ* visualisation of endogenous protein substrates of TG2, when combined with FITC-ExtrAvidin® (Lee *et al.* 1993). PACAP-27 (100 nM) induced a time dependent and concentration-dependent (EC_{50} = 6.7 ± 3 nM; pEC_{50} = 8.3 ± 0.2; n=3) increase in the incorporation of biotin-X-cadaverine into endogenous protein substrates of TG2 (Fig. 8). Finally, the *in situ* responses to PACAP-27 were attenuated by the PAC_1 antagonist PACAP 6-38 and the TG2 inhibitors ZDON and R283 (Fig. 8). Overall, these data indicate a similar pattern of TG2 activation in live cells.

3.6. *The role of Ca^{2+} in PAC_1 receptor induced TG2 activity*

PACAP-27 (100 nM) triggered a robust increase in intracellular Ca^{2+} that was abolished in the absence of extracellular Ca^{2+} (Fig. 9A and B). The role of extracellular Ca^{2+} in TG2 activation was assessed in the absence of extracellular Ca^{2+} using nominally Ca^{2+}-free Hanks/HEPES buffer containing 0.1 mM EGTA. Removal of extracellular Ca^{2+} abolished PACAP-27-induced TG2 activation (Fig. 9C and D). These observations suggest that PAC_1 receptor-induced TG2 activation is dependent upon extracellular Ca^{2+}.

3.7. *Phosphorylation of TG2 following PAC_1 receptor activation*

The effect of PAC_1 receptor activation on the phosphorylation status of TG2 was monitored via immunoprecipitation of TG2 followed by SDS-PAGE and Western blot analysis using anti-phosphoserine and anti-phosphothreonine antibodies. PACAP-27 (100 nM) triggered a robust increase in the levels of TG2 phosphoserine and phosphothreonine (Fig. 10). Pre-treatment with PD 98059 (50 μM; Fig. 10) and KT 5720 (5 μM; Fig. 11) attenuated PACAP-27 mediated increases in TG2 phosphorylation. In contrast, Ro 318220 (10 μM) had no significant effect (data not shown). Finally, removal of extracellular Ca^{2+} partially attenuated PACAP-27-induced TG2 phosphorylation (data not shown). These data indicate that activation of the PAC_1 receptor promotes robust increases in TG2 phosphorylation.

3.8. *Role of TG2 in PAC_1 receptor-induced cell survival and neurite outgrowth*

The role of TG2 in PAC_1 receptor-induced cell survival was determined in differentiating N2a cells following exposure of cells to simulated hypoxia (1% O_2 in glucose-free and serum-free medium). Initial experiments determined the time course of simulated hypoxia-induced cell death in differentiated N2a cells. Exposure of cells to simulated hypoxia (1% O_2) resulted in a time dependent decrease in MTT reduction, an increase in LDH release and activation of caspase 3 (Fig. 12). A time period of 8 h hypoxia was used in subsequent experiments. Pre-treatment with PACAP-27 (100 nM; 10 min) significantly attenuated hypoxia-induced decrease in MTT reduction, release of LDH and activation of caspase-3 (Fig. 13). Treatment with PACAP 6-38 (100 nM; 30 min) reversed PACAP-27 induced protection confirming the role of the PAC_1 receptor. Finally, the TG2 inhibitors R283 and Z-DON attenuated PACAP-27 induced cell survival (Fig. 14). To validate these observations in another cell model the role of TG2 in PAC_1 receptor-induced cell survival in human SH-SY5Y neuroblastoma cells was also investigated. Initial experiments demonstrated that PACAP-27 treatment produced transient increases in TG2 catalysed biotin-cadaverine incorporation and protein cross-linking activity, peaking at 30 min (Fig. 15A and C). Furthermore, as shown in Fig. 15, PACAP-27 stimulated concentration-dependent increases in biotin-amine incorporation activity (EC_{50} = 2.2 ± 1.0 nM; $p[EC_{50}]$ = 8.9 ± 0.4; n=3) and protein cross-linking activity (EC_{50} = 1.3 ± 0.5 nM; $p[EC_{50}]$ = 9.0 ± 0.2; n=3). Exposure of SH-SY5Y cells to simulated hypoxia (1% O_2) resulted in a time dependent decrease in MTT reduction, an increase in LDH release and activation of caspase 3 (data not shown), with 8 h used in subsequent experiments. As shown in Fig. 16, pre-treatment with PACAP-27 (100 nM; 10 min) significantly attenuated hypoxia-induced decrease in MTT reduction, release of LDH and activation of caspase-3 in SH-SY5Y cells (Fig. 16). Furthermore, PACAP 6-38 (100 nM; 30 min) reversed PACAP-27 induced protection confirming the role of the PAC_1 receptor in human SH-SY5Y cells (Fig. 16A to D). Finally, the TG2 inhibitors R283 and Z-DON attenuated PACAP-27 induced cell survival (Fig. 16E to G). Overall, these results demonstrate a role of TG2 in PAC_1 receptor-induced cell survival in both mouse N2a and human SH-SY5Y cells.

The role of TG2 in PAC_1 receptor induced neurite outgrowth was assessed by monitoring the outgrowth of axon-like processes following 24 and 48 h treatment with PACAP-27 (100 nM). The TG2 inhibitors Z-DON (150 μM) and R283 (200 μM) attenuated outgrowth of axon-like processes following 24 h (data not shown) and 48 h treatment with PACAP-27, confirming the involvement of TG2 (Fig. 17). These data confirm a role for TG2 in PAC_1 receptor mediated neurite outgrowth.

4. Discussion

The data in this report collectively suggest that PAC_1 receptor-mediated cell survival and neurite outgrowth are mediated by TG2, consistent with the view that TG2-mediated amine incorporation and protein cross-linking play important roles in these events.

4.1. In vitro modulation of TG2 transamidation activity by the PAC_1 receptor

Although the PAC_1 receptor is expressed in mitotic N2a cells (Leliévre *et al*., 1998; Miura *et al*., 2013) its functional expression in differentiating N2a cells has to our knowledge not been reported. Hence, this study has demonstrated for the first time functional expression of the PAC_1 receptor in N2a cells induced to differentiate with retinoic acid. The neuropeptide PACAP mediates neurite outgrowth and neuroprotection; however, it is not known if these events involve PAC_1 receptor-induced TG2 activation (Monaghan *et al*., 2008; Manecka *et al*., 2015; Jóźwiak-Bębenista *et al*., 2015). TG2 can catalyse two types of transamidation, namely (i) intra-, and/or inter-molecular covalent cross-links between protein-bound glutamine and protein-bound lysine residues, and (ii) cross-links between primary amines and protein-bound glutamine (Nurminskaya and Belkin, 2012). In this study the PAC_1 receptor agonist PACAP-27 triggered time- and concentration-dependent increases in TG2-mediated biotin-cadaverine incorporation and protein cross-linking activity in differentiating N2a cells. The EC_{50} values for PACAP-27 mediated transglutaminase-catalysed amine incorporation (0.08 nM) and protein cross-linking activity (0.4 nM) are in-line with the affinity of PACAP-27 for the PAC_1 receptor (Dickson *et al.,* 2006; Dickson and Finlayson, 2009; Harmar *et al*., 2012). Furthermore, PACAP-27-induced TG2 activity was blocked by the PAC_1 receptor antagonist PACAP 6-38 (Robberecht *et al*., 1992). Overall these data suggest that activation of TG2 by PACAP-27 is mediated via the PAC_1 receptor. It is important to note that PACAP 6-38 also displays high affinity for the $VPAC_2$ receptor (Dickinson *et al*.,1997); however, since the $VPAC_2$ agonist Bay 55-9837 did not trigger TG2 activity the effects of PACAP 6-38 are mediated entirely via the PAC_1 receptor. Finally, the PAC_1 receptor-induced increases in TG activity were inhibited by R283 and Z-DON, confirming that the observed increases in TG activity were via TG2.

At present, very little is known regarding the regulation of TG2 enzymic activity by GPCRs. Examples in the literature include muscarinic receptor-mediated increases in TG2 activity in SH-SY5Y cells (Zhang *et al*., 1998) and 5-HT_{2A} receptor-mediated transamidation (TG-catalyzed) of the small G-protein Rac1 in the rat cortical cell line A1A1v (Dai *et al*., 2008). The study by Zhang et al. (1998) measured *in situ* TG2 activity (polyamine incorporation) triggered by the non-selective muscarinic agonist carbachol, whereas, Dai et al. (2008) reported TG2 catalysed incorporation of 5-hydroxytryptamine into Rac1. 5-HT_{2A} receptor-mediated incorporation of 5-HT into the small GTPases RhoA

and Rab4 has also been observed in platelets (Walther *et al*., 2003). It was suggested that 5-HT_{2A} and muscarinic receptor-mediated release of Ca^{2+} from intracellular Ca^{2+} stores may be responsible for triggering TG transamidating activity (Zhang et al., 1998; Walther *et al*., 2003). Our recent studies have shown that the $G_{i/o}$-protein coupled A_1 adenosine receptor stimulates TG2 activation in H9c2 cardiomyocyte-like cells (Vyas *et al*., 2016). Since TG2 transamidase activity modulates protein function by cross-linking and incorporation of small molecule mono- and polyamines into protein substrates, it is likely that activation of TG2 by GPCRs plays a major role in the regulation of cellular function (Nurminskaya and Belkin, 2012; Eckert *et al*., 2014).

4.2. Role of Ca^{2+} in PAC_1 receptor-mediated TG2 activation

The transamidating activity of TG2 is dependent upon Ca^{2+}, which promotes the "open" form of TG2 and negates the inhibitory actions of the nucleotides GTP, GDP and ATP (Király *et al*., 2011). Previous studies have shown that release of Ca^{2+} from intracellular Ca^{2+} stores or influx of extracellular Ca^{2+} is linked to TG activation in response to GPCR stimulation (Zhang *et al*., 1998; Walther *et al*., 2003; Vyas *et al*., 2016). The data presented in the current work indicate that PAC_1 receptor-induced transamidase activity is dependent upon extracellular Ca^{2+}. Previous studies have shown that the PAC_1 receptor promotes Ca^{2+} mobilization from intracellular stores and Ca^{2+} influx via N-type calcium channels (Basille-Dugay *et al*., 2013) in rat cerebellar granule cells. In this study, PACAP-27-triggered Ca^{2+} responses were abolished in the absence of extracellular Ca^{2+} , which is indicative of Ca^{2+} influx. Clearly, further studies are required to determine the mechanism(s) of PAC_1 receptor-induced Ca^{2+} influx in differentiated N2a cells and its role in TG2 activation. It is interesting to note that changes in intracellular [Ca^{2+}] required for TG2 transamidating activity are typically in the order 3-100 μM (Király *et al*., 2011). However, there is growing evidence that intracellular [Ca^{2+}] can reach levels sufficient to activate TG2, for example in calcium microdomains that occur near the cell membrane following the opening of voltage gated Ca^{2+} channels or near internal stores (Berridge, 2006; Király *et al*., 2011). Alternatively, the role of Ca^{2+} in PAC_1 receptor-induced TG2 activation may require the sensitization of TG2 to low levels of intracellular [Ca^{2+}]. For example, interaction of TG2 with protein binding partners and/or membrane lipids have been proposed to induce a conformational change that promotes activation at low levels of intracellular [Ca^{2+}] (Király *et al*., 2011).

4.3. Role of protein kinases in PAC_1 receptor-mediated TG2 activation

The phosphorylation of TG2 by PKA inhibits its transamidating activity but augments its kinase activity (Mishra *et al.* 2007). These contrasting effects on TG2 activity were obtained using histidine-tagged TG2 immobilized on nickel-agarose and incubated with

the catalytic subunit of PKA. In this study the PKA inhibitors KT 5720 and *Rp*-cAMPs completely blocked PACAP-27-induced TG2 transamidating activity, which reflects PAC_1 receptor signaling via cAMP/PKA. The PAC_1 receptor also activates PLC/DAG/PKC (via G_q-protein coupling) signalling and hence we determined the role of PKC. The broad spectrum PKC inhibitor Ro 318220 inhibited PACAP-27-induced TG2 activity, indicating that G_q-protein coupling is involved in PAC_1 receptor-mediated TG2 activation. The PAC_1 receptor also activates ERK1/2, JNK1/2, p38 MAPK and PKB (Monaghan *et al*., 2008; May *et al*., 2010, Castorina *et al*., 2014). In this study we observed PACAP-27-induced activation of ERK1/2, JNK1/2, and PKB but not p38 MAPK. The MEK1/2 (upstream activator of ERK1/2) inhibitor PD 98059 blocked PACAP-27-induced TG2 activity, suggesting a prominent role for ERK1/2. These observations are comparable to A_1 adenosine receptor-mediated activation of TG2 in H9c2 cells, which was also sensitive to PKC and ERK1/2 inhibition (Vyas *et al*., 2016). In transfected HEK293 cells, PAC_1 receptor-induced ERK1/2 is dependent upon calcium influx and PLC/DAG/PKC (May *et al*., 2014) and hence the inhibition of PACAP-27-induced TG2 by removal of extracellular Ca^{2+} and inhibition of PKC may reflect their up-stream role(s) in ERK1/2 activation. In the current study, PAC_1 receptor-induced ERK1/2 activation is independent of Ca^{2+} influx and partially sensitive to PKC inhibition. Similarly, PKA can activate ERK1/2 (Stork and Schmitt, 2002) and therefore the effect of PKA inhibitors on PAC_1 receptor TG2 activation may also reflect the up-stream role of PKA in ERK1/2 activation. In SH-SY5Y cells PAC_1 receptor-induced ERK1/2 activation is cAMP-dependent but PKA-independent (Monaghan *et al*., 2008). However, in guinea-pig cardiac neurons (Clason *et al*., 2016) and N2a cells (the current study) PAC_1 receptor-induced ERK1/2 signalling is PKA-dependent. Hence, PKA-mediated inhibition of TG2 activation may indeed reflect the up-stream role of PKA in ERK1/2 activation. Finally, PACAP-27-induced TG2 activation was also sensitive to inhibition of PKB and JNK1/2, suggesting a role for these kinases in PAC_1 receptor-induced TG2 activation.

We have previously shown that TG2 is phosphorylated following activation of the A_1 adenosine receptor in H9c2 cells (Vyas *et al*., 2016). The current data demonstrate that TG2 is also phosphorylated following PAC_1 receptor activation. Furthermore, PAC_1 receptor-induced TG2 phosphorylation was attenuated by pharmacological inhibition of MEK1/2, PKA and removal of extracellular Ca^{2+}. It is not clear how the absence of extracellular Ca^{2+} blocks TG2 phosphorylation since PAC_1 receptor-induced ERK1/2 activation is independent of Ca^{2+} influx. One possible explanation is that changes in $[Ca^{2+}]_i$ promote conformational changes in TG2 that facilitate its phosphorylation by protein kinase(s). Alternatively, Ca^{2+} influx may play a role in augmenting PAC_1 receptor-induced PLC/PKC signalling. However, the fact that the PKC inhibitor Ro 31-8220 did not block TG2 phosphorylation, suggests that PKC may regulate other targets

involved in TG2 activation. The next logical step would be to identify the specific site(s) of TG2-associated serine and threonine phosphorylation. Previous studies have shown that TG2 is phosphorylated by PKA at Ser^{215} and Ser^{216} (Mishra and Murphy, 2006) and at an unknown site(s) by PTEN-induced putative kinase 1 (PINK1; Min et al., 2015). At present the precise role of PAC_1 receptor-induced TG2 phosphorylation is not known. However, PKA-mediated phosphorylation of TG2 enhances its interaction with the scaffolding protein 14-3-3 and increases TG2 kinase activity, whereas PINK1-mediated phosphorylation of TG2 blocks its proteasomal degradation (Mishra and Murphy, 2006; Mishra et al., 2007; Min et al., 2015). It is also conceivable that TG2 phosphorylation sensitizes TG2 to low levels of intracellular [Ca^{2+}] or alters its subcellular location. Work underway will determine the functional consequences of PAC_1 receptor-induced TG2 phosphorylation.

4.4 In situ visualisation of TG2 activity

Fluorescence microscopy was used to visualise *in situ* TG2 activity following PAC_1 receptor activation. The results were comparable to PAC_1 receptor-induced amine incorporation activity observed *in vitro*. However, given the covalent nature of biotin-X-cadaverine incorporation into protein substrates, it was surprising to observe that *in situ* TG2 activity returned to basal levels after 40 min. Possible explanations for this include reversal of amine incorporation by TG (Stamnaes *et al*. 2008), targeting of modified proteins for degradation or their rapid removal from the cell. Our previous studies have reported the rapid expulsion of biotinylated proteins from H9c2 cells following treatment with PMA or forskolin (Almami *et al*. 2014). It could be that the rapid expulsion of biotinylated proteins from N2a cells occurs via exosomes (Kalani *et al*. 2014). Since N2a cells secrete exosomes it will be interest to determine whether amine-labelled proteins can be detected in exosomes purified from cell culture supernatants obtained from these cells following PACAP-27 treatment (Chivet *et al*. 2014).

4.5. Role of TG2 in PAC_1 receptor-induced cytoprotection

Previous studies have shown that TG2 protects human SH-SY5Y neuroblastoma cells against heat shock–induced cell death (Tucholski *et al*., 2001). Similarly, TG2 mediates protection of neuronal cells against hypoxia and oxygen/glucose deprivation–induced cell death by attenuating the HIF hypoxic response pathway (Filiano *et al*. 2008). Likewise, PACAP is widely recognized as a neuroprotective peptide and potential therapeutic agent for the treatment of cerebral ischaemia and various neurodegenerative disorders (Reglodi *et al*., 2011; Lee and Seo, 2014). The mechanisms of PACAP/PAC_1 receptor-induced neuroprotection are complex and involve multiple signalling pathways that include PKA, PKB, ERK1/2, NF-κB and Ca^{2+} mobilization (May *et al*., 2010; Baxter *et al*.,

2011; Manecka *et al*., 2013). In this study we have shown for the first time a role for TG2 in PAC_1 receptor-induced cytoprotection in differentiating mouse N2a and human SH-SY5Y neuroblastoma cells. However, whilst it is not clear how PAC_1 receptor-induced TG2 activation mediates cell survival, TG2 is known to regulate pathways associated with PACAP neuroprotection. For example, TG2 activates adenylyl cyclase and enhances cAMP/PKA dependent CRE-reporter gene activity in SH-SY5Y neuroblastoma cells (Tucholski and Johnson, 2003) and promotes NF-κB signaling via cross-linking of IκBα (Erkert *et al*., 2014). In the current study inhibition of TG2 blocked PACAP-27 mediated attenuation of hypoxia-induced activation of caspase-3. Recent studies have shown that TG2 inhibits apoptosis via the down-regulation of the Bax expression and inhibition of caspase 3 and 9 (Cho *et al*., 2010). Further work is required to determine the role of TG2 in PAC_1 receptor-induced cell survival.

4.6. *Role of TG2 in PAC_1 receptor-induced neurite outgrowth*

Previous studies have shown that TG2 is essential for differentiation/neurite outgrowth in human neuroblastoma SHSY5Y cells (Tucholski *et al*., 2001; Singh *et al*., 2003). Mechanisms associated with TG2-induced neurite outgrowth include transamidation of RhoA and subsequent activation of ERK1/2 and p38 MAPK (Singh *et al*., 2003). Similarly, PACAP triggers neuronal differentiation of human SH-SY5Y cells via a cAMP-dependent but PKA-independent pathway requiring activation of ERK1/2 and p38 MAPK (Monaghan *et al*. 2008). The data presented in this study suggest that pharmacological inhibition of TG2 blocks PACAP-27-induced outgrowth of axon-like processes, suggesting the involvement of TG2 in PAC_1 receptor neurite outgrowth. However, further studies are required to identify the downstream substrates of TG2 and signalling pathways associated with the role of TG2 in PAC_1 receptor neuronal differentiation.

In conclusion, our data show for the first time that TG2 activity is regulated by the PAC_1 receptor in differentiating N2a and SH-SY5Y cells. Work is currently underway to understand more fully the role of TG2 in PAC_1 receptor signalling and modulation of neuronal cell function.

Acknowledgements and conflicts of Interest

This work was supported by a PhD studentship from the Saudi Arabian Government (UMU473) We would like to thank Gordon Arnott for help with confocal imaging. The authors state no conflict of interest.

Figure legends

Figure 1. Protein expression of TG isoforms and neuronal markers in mitotic and differentiated N2 cells. Where indicated cells were differentiated with retinoic acid (1 μM) or PACAP-27 (100 nM) for 48 h in serum-free medium. (A) Immunocytochemistry by fluorescence microscopy was performed using anti-choline acetyltransferase antibody (ChAT; cholinergic neuronal marker; green) and anti-tyrosine hydroxylase antibody (TH; dopaminergic and noradrenergic neuronal marker) and DAPI counterstain for nuclei visualisation (blue). Images presented are from one experiment and representative of three. (B) Quantified immunocytochemistry data represent the mean ± S.E.M. of fluorescence intensity relative to DAPI stain for five fields of view each from three independent experiments. (C) Cell lysates (20 μg protein) from mitotic (M) and differentiating (D) N2a cells were analysed for TG1, TG2 and TG3 expression by Western blotting using TG isoform specific antibodies. Levels of GAPDH are included for comparison. (D) Quantified data are expressed as the ratio of TG isoform to GAPDH and represent the mean ± S.E.M. from four independent experiments. $^{**}P<0.01$, $^{***}P<0.001$, and $^{****}P<0.0001$ *versus* mitotic cells.

Figure 2: PACAP-27-induced cAMP accumulation in differentiating N2a cells. Differentiating N2a cells were treated with the indicated concentrations of PACAP-27 for 10 min. Levels of cAMP were determined as described in Materials and Methods. The results represent the mean ± S.E.M. of three experiments each performed in triplicate. $^{*}P<0.05$, $^{**}P<0.01$, and $^{****}P<0.0001$ *versus* control response.

Figure 3. Effect of PACAP-27 on transglutaminase activity in N2a cells. Differentiating N2a cells were either incubated with 100 nM PACAP-27 for the indicated time periods or for 10 min with the indicated concentrations of PACAP-27. Cell lysates were then subjected to the biotin-cadaverine incorporation (A and B) or protein cross-linking assay (C and D). Data points represent the mean TG specific activity ± S.E.M. from four (A and C), five (B) or six (D) independent experiments. $^{*}P<0.05$, $^{**}P<0.01$, $^{***}P<0.001$, and $^{****}P<0.0001$ *versus* control response.

Figure 4. Effect of the selective PAC_1 receptor antagonist PACAP 6-38 and inhibitors of TG2 and PKA in on PACAP-27 induced TG2 activity in differentiating N2a cells. Cells were

pretreated for 1 h with the TG2 inhibitors Z-DON (150 μM) and R283 (200 μM) or for 30 min with the selective PAC_1 receptor antagonist PACAP 6-38 (100 nM) or the PKA inhibitors KT 5720 (5 μM) or Rp-3',5'-cAMPs (50 μM) prior to 10 min stimulation with PACAP-27 (100 nM). Cell lysates were then subjected to the biotin-cadaverine incorporation (A,C,E) or protein cross-linking assay (B,D,F). Data points represent the mean TG specific activity ± S.E.M. from four independent experiments. *P<0.05, ***P<0.001, and ****P<0.0001, (a) versus control and (b) versus 100 nM PACAP-27 alone.

Figure 5. Effect of PACAP-27 on ERK1/2, PKB and JNK1/2 phosphorylation in differentiating N2a cells. Where indicated, N2a cells were pre-treated for 30 min with PD 98059 (50 μM), SP 600 125 (20 μM) or Akt inhibitor X1 (100 nM, 1 μM or 10 μM) prior to stimulation with PACAP-27 (100 nM) for 10 min. Cell lysates were analysed by Western blotting for activation of (A) ERK1/2, (B) PKB and (C) JNK1/2 using phospho-specific antibodies. Samples were subsequently analysed on separate blots using antibodies that recognize total ERK1/2, PKB and JNK1/2. Quantified data are expressed as the percentage of the value for control cells (=100%) in the absence of protein kinase inhibitor and represent the mean ± S.E.M. of four independent experiments. ***P<0.001 and ****P<0.0001, (a) versus control and (b) versus 100 nM PACAP-27.

Figure 6. Effect of protein kinase inhibitors (PKA, PKC) and Ca^{2+} on PACAP-27 induced ERK1/2 activation. Where indicated, differentiating N2a cells were pre-treated for 30 min with (A) KT 5720 (5 μM) or (B) Ro 318220 (10 μM) prior to stimulation with PACAP-27 (100 nM) for 10 min. (C) cells were stimulated for 10 min with PACAP-27 (100 nM) either in the presence (1.8 mM $CaCl_2$) or absence of extracellular Ca^{2+} (nominally Ca^{2+}-free Hanks/HEPES buffer containing 0.1 mM EGTA). Cell lysates were analysed by Western blotting for activation of ERK1/2 using a phospho-specific antibody. Samples were subsequently analysed on separate blots using an antibody that recognizes total ERK1/2. Quantified data are expressed as the percentage of the value for control cells (=100%) in the absence of protein kinase inhibitor or presence of extracellular Ca^{2+} and represent the mean ± S.E.M. of four independent experiments. ***P<0.001 and ****P<0.0001, (a) versus control and (b) versus 100 nM PACAP-27.

Figure 7. Effect of protein kinase inhibitors (ERK1/2, PKC, PKB, JNK1/2) on PAC_1 receptor-induced TG activity. Differentiating N2a cells were pretreated for 30 min with PD 98059 (50 μM), Ro 31-8220 (10 μM), Akt inhibitor XI (100 nM) or SP 600125 (20 μM)

prior to 10 min stimulation with PACAP-27 (100 nM). Cell lysates subjected to biotin-cadaverine incorporation (A,C,E) or protein cross-linking assay (B,D,F). Data points represent the mean ± S.E.M. TG specific activity from four independent experiments. *P<0.05, ** P<0.01, *** P<0.001 and **** P<0.0001, (a) versus control and (b) versus 100 nM PACAP-27 alone.

Figure 8. PACAP-27-induced *in situ* TG activity in differentiating N2a cells. Cells were incubated with 1 mM biotin-X-cadaverine (BTC) for 6 h, after which they were incubated with (A) 100 nM PACAP-27 for 5, 10, 20, or 40 min, (B) the indicated concentrations of PACAP-27 for 10 min, or (C) with the PAC_1 receptor antagonist PACAP 6-38 (100 nM) for 30 min or for 1 h with the TG2 inhibitors Z-DON (150 μM) and R283 (200 μM) prior to 10 min stimulation with PACAP-27 (100 nM). TG2-mediated biotin-X-cadaverine incorporation into intracellular proteins was visualized using FITC-conjugated ExtrAvidin® (green). Nuclei were stained with DAPI (blue) and viewed using a Leica TCS SP5 II confocal microscope (20x objective magnification). Images presented are from one experiment and representative of three. Quantified data represent the mean ± S.E.M. of fluorescence intensity relative to DAPI stain for five fields of view each from at least three independent experiments. *P<0.05, ** P<0.01, *** P<0.001 and ****P<0.0001 versus control response.

Figure 9. Effect of PACAP-27 on $[Ca^{2+}]_i$ and role of Ca^{2+} in PACAP-27-induced TG2 activation in differentiating N2a cells. Shown are A) PACAP-27 (100 nM) triggering a rapid and transient rise in intracellular Ca^{2+} in the presence of extracellular Ca^{2+} (1.3 mM). B) the absence of Ca^{2+} responses induced by PACAP-27 during experiments performed in nominally Ca^{2+}-free buffer and 0.1 mM EGTA. In these experiments depletion of intracellular Ca^{2+} stores with thapsigargin (5 μM) was still evident. The panel letters (a-d) correspond to the time points in the traces. Similar results were obtained in three other experiments. For TG2 activity, cells were stimulated for 10 min with PACAP-27 (100 nM) either in the presence (1.8 mM $CaCl_2$) or absence of extracellular Ca^{2+} (nominally Ca^{2+}-free Hanks/HEPES buffer containing 0.1 mM EGTA). Cell lysates were subjected to biotin-cadaverine incorporation assay (C) or protein cross-linking assay (D). Data points represent the mean TG specific activity ± S.E.M. from four independent experiments. ** P<0.01, *** P<0.001 and **** P<0.0001, (a) versus control in presence of extracellular Ca^{2+}, (b) versus 100 nM PACAP-27 in presence of extracellular Ca^{2+}.

Figure 10. Effect of the MEK1/2 inhibitor PD 98059 on PACAP-27-induced phosphorylation of TG2. Where indicated, differentiating N2a cells were pre-treated for 30 min with PD 98059 (50 μM) prior to stimulation with PACAP-27 (100 nM) for 10 min. Following stimulation with PACAP-27, cell lysates were subjected to immunoprecipitation using anti-TG2 monoclonal antibody as described under " Materials and Methods". The resultant immunoprecipitated protein(s) were subjected to SDS-PAGE and Western blot analysis using (A) anti-phosphoserine and (B) and anti-phosphothreonine antibodies. One tenth of the total input was applied to the first lane to show the presence of phosphorylated proteins prior to immunoprecipitation and negative controls with the immunoprecipitation performed with immunobeads only were included to demonstrate the specificity of the band shown. Quantified data for PACAP-induced increases in TG2-bound serine and threonine phosphorylation are expressed as a percentage of the TG2 phosphorylation observed in control cells (=100%). Data points represent the mean ± S.E.M. from three independent experiments. $*P<0.05$, $**P<0.01$, and $***P<0.001$, (a) versus control and (b) versus 100 nM PACAP-27 alone.

Figure 11. Effect of the PKA inhibitor KT 5720 on PACAP-27-induced phosphorylation of TG2. Where indicated, differentiating N2a cells were pre-treated for 30 min with KT 5720 (5 μM) prior to stimulation with PACAP-27 (100 nM) for 10 min. Following stimulation with PACAP-27, cell lysates were subjected to immunoprecipitation using anti-TG2 monoclonal antibody as described under " Materials and Methods". The resultant immunoprecipitated protein(s) were subjected to SDS-PAGE and Western blot analysis using (A) anti-phosphoserine and (B) and anti-phosphothreonine antibodies. One tenth of the total input was applied to the first lane to show the presence of phosphorylated proteins prior to immunoprecipitation and negative controls with the immunoprecipitation performed with immunobeads only were included to demonstrate the specificity of the band shown. Quantified data for PACAP-induced increases in TG2-bound serine and threonine phosphorylation are expressed as a percentage of the TG2 phosphorylation observed in control cells (=100%). Data points represent the mean ± S.E.M. from three independent experiments. $*P<0.05$, $**P<0.01$, and $***P<0.001$, (a) versus control and (b) versus 100 nM PACAP-27 alone.

Figure 12. Effect of simulated hypoxia on MTT reduction, LDH release and caspase 3 activity in differentiating N2a cells. Cells in glucose- and serum-free DMEM were exposed to hypoxia (1% O_2) for the indicated periods of time. Cell viability was assessed by

measuring (A) the metabolic reduction of MTT by cellular dehydrogenases, (B) release of LDH into the culture medium and (C) caspase-3 activity via Western blot analysis using anti-active caspase 3 antibody. (D) Quantified caspase-3 activity data. Data are expressed as the percentage of the normoxic control (=100%) and represent the mean ± S.E.M. from four independent experiments, each performed in (A) quadruplicate or (B) sextuplicate. *P<0.05, ***P<0.0001 and **** p<0.0001 *versus* normoxic control.

Figure 13. The effect of PACAP-27 on hypoxia-induced cell death in N2a cells. Differentiating N2a cells were pre-treated with the PAC_1 receptor antagonist PACAP 6-38 (100 nM) for 30 min before the addition of PACAP-27 (100 nM) for 10 min prior to 8 h hypoxia (1% O_2) or 8 h normoxia. Cell viability was assessed by measuring (A) the metabolic reduction of MTT by cellular dehydrogenases, (B) release of LDH into the culture medium and (C) caspase-3 activity via Western blot analysis using anti-active caspase 3 antibody. (D) Quantified caspase-3 activity data. Data are expressed as a percentage of normoxia control cell values (=100%) and represent the mean ± S.E.M. from four independent experiments, each performed in (A) quadruplicate or (B) sextuplicate. ****P<0.0001, (a) versus normoxia control, (b) versus hypoxia control (c) versus 100 nM PACAP-27 in the presence of hypoxia.

Figure 14. The effects of the TG2 inhibitors Z-DON and R283 on PACAP-27 induced cell survival in N2a cells. Differentiating N2a cells were pre-treated for 1 h with the TG2 inhibitors Z-DON (150 μM) or R283 (200 μM) before the addition of PACAP-27 (100 nM) for 10 min prior to 8 h hypoxia (1% O_2) or 8 h normoxia. Cell viability was assessed by measuring (A) the metabolic reduction of MTT by cellular dehydrogenases, (B) release of LDH into the culture medium and (C) caspase-3 activity via Western blot analysis using anti-active caspase 3 antibody. (D) Quantified caspase-3 activity data. Data are expressed as a percentage of normoxia control cell values (=100%) and represent the mean ± S.E.M. from four independent experiments each performed in (A) quadruplicate and (B) sextuplicate. *P<0.05, **P<0.01, ***P<0.0001 and ****P<0.0001, (a) versus normoxia control, (b) versus hypoxia control (c) versus 100 nM PACAP-27 in the presence of hypoxia.

Figure 15. Effect of PACAP-27 on transglutaminase activity in human SH-SY5Y neuroblastoma cells. Differentiating SH-SY5Y cells were either incubated with 100 nM PACAP-27 for the indicated time periods or for 30 min with the indicated concentrations of PACAP-27. Cell lysates were then subjected to the biotin-cadaverine incorporation (A and B) or protein cross-linking assay (C and D). Data points represent the mean TG

specific activity ± S.E.M. from four (A and C) or three (B and D) independent experiments. *P<0.05, **P<0.01, ***P<0.001, and ****P<0.0001 *versus* control response.

Figure 16. The effect of PACAP-27 on hypoxia-induced cell death in human SH-SY5Y cells. Differentiating SH-SY5Y cells were pre-treated either with the PAC_1 receptor antagonist PACAP 6-38 (100 nM) for 30 min (panels A-D) or with the TG2 inhibitors Z-DON (150 µM) or R283 (200 µM) for 1 h (panels E-H) before the addition of PACAP-27 (100 nM) for 10 min prior to 8 h hypoxia (1% O_2) or 8 h normoxia. Cell viability was assessed by measuring the metabolic reduction of MTT by cellular dehydrogenases (panels A,E), release of LDH into the culture medium (panels B,F) and caspase-3 activity via Western blot analysis using anti-active caspase 3 antibody (panels C,G). Quantified caspase-3 activity data is shown in panels D and H. Data are expressed as a percentage of normoxia control cell values (=100%) and represent the mean ± S.E.M. from four independent experiments each performed in (A,E) quadruplicate and (B,F) sextuplicate. *P<0.05, **P<0.01, $^{***}P$<0.0001 and ****P<0.0001, (a) versus normoxia control, (b) versus hypoxia control (c) versus 100 nM PACAP-27 in the presence of hypoxia.

Figure 17. The effect of TG2 inhibitors on PACAP-27 induced outgrowth of axon-like processes in differentiating N2a cells. (A) N2a cells were incubated for 1 h with the TG2 inhibitors Z-DON (150 µM) or R283 (200 µM) before treatment with PACAP-27 (100 nM) in serum-free DMEM for 48 h. Following stimulation the cells were fixed and stained with Coomassie blue. (B) Quantified data points represent the number of axon-like processes determined as described in Materials and Methods. Shown are the mean number of axons/100 cells ± S.E.M. from four independent experiments each performed in quadruplicate. White arrows indicate typical axon-like processes. $^{***}P$<0.0001 and ****P<0.0001, (a) versus mitotic control, (b) versus 100 nM PACAP-27 alone.

References

Almami I, Dickenson JM, Hargreaves AJ, Bonner PLR (2014) Modulation of transglutaminase 2 activity in H9c2 cells by PKC and PKA signalling: a role for transglutaminase 2 in cytoprotection. *Br. J. Pharmacol.* **171,** 3946-3960.

Barve V, Ahmed F, Adsule S, Banerjee S, Kulkarni S, Katiyar P et al. (2006) Synthesis, molecular characterization, and biological activity of novel synthetic derivatives of chromen-4-one in human cancer cells. *J Med Chem* **49:** 3800-3808.

Basille-Dugay M, Vaudry H, Fournier A, Gonzalez B, Vaudry D (2013) Activation of PAC1 receptors in rat cerebellar granule cells stimulates both calcium mobilization from intracellular stores and calcium influx through N-type calcium channels. *Front Endocrinol*. **4,** 56.

Baxter PS, Martel M-A, McMahon A, Kind PC, Hardingham GE (2011) Pituitary adenylate cyclase-activating peptide induces long-lasting neuroprotection through the induction of activity-dependent signaling via the cyclic AMP response element-binding protein-regulated transcription co-activator 1. *J. Neurochem.* **118,** 365-378.

Bennett BL, Sasaki DT, Murray BW, O'Leary EC, Sakata ST, Xu W *et al*. (2001) SP 600125, an anthrapyrazolone inhibitor of Jun N-terminal kinase. *Proc Natl Acad Sci* USA **98:** 13681-13686.

Berridge MJ (2006) Calcium microdomains: organization and function. *Cell Calcium* **40,** 405-412.

Bollag WB, Zhong X, Dodd EM, Hardy DM, Zheng X, Allred WT (2005) Phospholipase D signaling and extracellular signal-regulated kinase-1 and -2 phosphorylation (activation) are required for maximal phorbol-ester-induced transglutaminase activity, a marker of keratinocyte differentiation. *J. Pharmacol. Expt. Ther*. **312,** 1223-1231.

Castorina A, Scuderi S, D'Amico AG, Drago F, D'Agata V (2014) PACAP and VIP increase the expression of myelin-related proteins in rat schwannoma cells: involvement of PAC1/VPAC2 receptor-mediated activation of PI3K/Akt signaling pathways. *Exp. Cell Res*. **322,** 108-121.

Chivet M, Javalet C, Laulagnier K, Blot B, Hemming FJ, Sadoul R (2014) Exosomes secreted by cortical neurons upon glutamatergic synapse activation specifically interact with neurons. *J. Extracell. Vesicles* **3,** 24722 doi: 10.3402/jev.v3.24722.

Cho SY, Lee JH, Bae HD, Jeong EM, Jang GY, Kim CW, Shin DM, Jeon JH, Kim IG (2010) Transglutaminase 2 inhibits apoptosis induced by calcium-overload through down-regulation of Bax. *Exp. Mol. Med.* **42,** 639-650.

Clason TA, Girard BM, May V, Parsons RL (2016) Activation of MEK/ERK signaling by PACAP in guinea pig cardiac neurons. *J. Mol. Neurosci.* 59: 309-316.

Condello S, Caccamo D, Currò M, Ferlazzo N, Parisi G, Ientile R (2008) Transglutaminase 2 and NF-κB interplay during NGF-induced differentiation of neuroblastoma cells. *Brain Res.* **1207,** 1-8.

Dai Y, Dudek NL, Patel TB, Muma NA (2008) Transglutaminase-catalysed transmidation: a novel mechanism for Rac1 activation by 5-hydroxytryptamine$_{2A}$ receptor stimulation. *J. Pharmacol. Expt. Ther*. **326,** 153-162.

de Wit RJ, Hekstra D., Jastorff B, Stec WJ, Baraniak J, Van Driel R, Van Haastert PJ (1984) Inhibitory action of certain cyclophosphate derivatives of cAMP on cAMP-dependent protein kinases. *Eur J Biochem* **142:** 255-260.

Dickinson T, Fleetwood-Walker SS, Mitchell R, Lutz EM (1997) Evidence for roles of vasoactive intestinal polypeptide (VIP) and pituitary adenylate cyclase activating polypeptide (PACAP) receptors in modulating the responses of rat dorsal horn neurons to sensory inputs. *Neuropeptides* **31,** 175-185.

Dickson L, Aramori I, McCulloch J, Sharkey J, Finlayson K (2006) A systematic comparison of intracellular cyclic AMP and calcium signalling highlights complexities in human VPAC/PAC receptor pharmacology. *Neuropharmacol* **51:** 1086-1098.

Dickson L, Finlayson K (2009) VPAC and PAC receptors: from ligands to function. *Pharmacol. Ther.* **121,** 294-316.

Dudley DT, Pang L, Decker SJ, Bridges AJ, Saltiel AR (1995) A synthetic inhibitor of the mitogen-activated protein kinase cascade. *Proc Natl Acad Sci* USA **92:** 7686-7689.

Eckert RL, Kaartinen MT, Nurminskaya M, Belkin AM, Colak G, Johnson GVW, Mehta K (2014) Transglutaminase regulation of cell function. *Physiol. Rev.* **94,** 383-417.

Filiano AJ, Bailey CDC, Tucholski J, Gundemir S, Johnson GVW (2008) Transglutaminase 2 protects against ischemic insult, interacts with HIF1β, and attenuates HIF1 signaling. *FASEB J*. **22,** 2662-2675.

Filiano AJ, Tucholski J, Dolan PJ, Colak G, Johnson GVW (2010) Transglutaminase 2 protects against ischemic stroke. *Neurobiol. Dis.* **39,** 334-343.

Frampton G, Invernizzi P, Bernuzzi F, Pae HY, Quinn M, Horvat D, Galindo C, Huang L, McMillin M, Cooper B, Rimassa L, DeMorrow S (2012) Interleukin-6-driven progranulin expression increases cholangiocarcinoma growth by an Akt-dependent mechanism. *Gut* **61:** 268-277.

Freund KF, Doshi KP, Gaul SL, Claremon DA, Remy DC, Baldwin JJ *et al*. (1994) Transglutaminase inhibition by 2-[(2-oxopropyl)thio]imidazolium derivatives: mechanism of factor XIIIa inactivation. *Biochemistry* **33,** 10109-10119.

Gundemir S, Colak G, Tucholski J, Johnson GVW (2012) Transglutaminase 2: a molecular Swiss army knife. *Biochim. Biophys. Acta.* **1823,** 406-419.

Hah YS, Kang HG, Cho HY, Shin SH, Kim UK, Park BW, Lee SI, Rho GJ, Kim JR, Byun JH (2013) JNK signaling plays an important role in the effects of TNF-α and IL-1β on in vitro osteoblastic differentiation of cultured human periosteal-derived cells. *Mol Biol Rep* **40:** 4869-4881.

Hargreaves AJ, Fowler MJ, Sachana M, Flaskos J, Bountouri M, Coutts IC et al (2006) Inhibition of Neurite Outgrowth in Differentiating Mouse N2a Neuroblastoma Cells by Phenyl Saligenin Phosphate: Effects on MAP Kinase (ERK 1/2) Activation, Neurofilament Heavy Chain Phosphorylation and Neuropathy Target Esterase Activity. *Biochem. Pharmacol.* **71,** 1240–1247.

Harmar AJ, Fahrenkrug J, Gozes I, Laburthe M, May V, Pisegna JR, Vaudry D, Vaudry H, Waschek JA, Said SI (2012) Pharmacology and functions of receptors for vasoactive intestinal peptide and pituitary adenylate-activating polypeptide: IUPHAR Review 1. *Br. J. Pharmacol. 166,* 4-17.

Jóźwiak-Bębenista M, Kowalczyt E, Nowak JZ (2015) The cyclic AMP effects and neuroprotective activities of PACAP and VIP in cultured astrocytes and neurons exposed to oxygen-glucose deprivation. *Pharmacol. Reports* **67,** 332-338.

Kalani A, Tyagi A, Tyagi N (2014) Exosomes: mediators of neurodegeneration, neuroprotection and therapeutics. *Mol. Neurobiol.* **49,** 590-600.

Kase H, Iwahashi K, Nakanishi S, Matsuda Y, Yamada K, Takahashi M et al (1987) K-252 compounds, novel and potent inhibitors of protein kinase C and cyclic nucleotide-dependent protein kinases. Biochem *Biophys Res Commun* **142:** 436-440.

Kim JH, Lee SC, Ro J, Kang HS, Kim HS, Y S (2010) Jnk signaling pathway-mediated regulation of Stat3 activation is linked to the development of doxorubicin resistance in cancer cell lines. *Biochem Pharmacol* **79:** 373-380.

Kim YH, Lee DH, Jeong JH, Guo ZS, Lee YJ (2008) Quercetin augments TRAIL-induced apoptotic death: involvement of the ERK signal transduction pathway. *Biochem Pharmacol* **75:** 1946-1958.

Király R, Demény MA, and Fésüs L (2011) Protein transamidation by transglutaminase 2 in cells: a disputed Ca^{2+}-dependent action of a multifunctional protein *FEBS J*. **278,** 4717-4739.

Keilbaugh SA, Prusoff WH, Simpson MV (1991) The PC12 cell as a model for studies of the mechanism of induction of peripheral neuropathy by anti-HIV-I dideoxynucleoside analogs. *Biochem. Pharmacol.* **42,** R5-R8.

Lee EH, Seo SR (2014) Neuroprotective role of pituitary adenylate cyclase-activating polypeptide in neurodegenerative diseases. *BMB Rep.* **47,** 369-375.

Lee IT, Lin CC, Wang CH, Cherng WJ, Wang JS, Yang CM (2013) ATP stimulates PGE_2/cyclin D1-dependent VSMCs proliferation via STAT3 activation: role of PKCs-dependent NADPH oxidase/ROS generation. *Biochem Pharmacol* **85:** 954-964.

Lee KN, Arnold SA, Birkbichler PJ, Patterson Jr MK, Fraij BM, Takeuchi Y, Carter HA (1993) Site-directed mutagenesis of human tissue transglutaminase: Cys-277 is essential for transglutaminase activity but not for GTPase activity. *Biochim. Biophys. Acta.* **1202,** 1-6.

Leliévre V, Pineau N, Du J, Wen C-H, Nguyen T, Janet T et al (1998) Differential effects of peptide histidine isoleucine (PHI) and related peptides on stimulation and suppression of neuroblastoma cell proliferation. *J. Biol. Chem*. **273,** 19685-19690.

Lilley GR, Skill J, Griffin M, Bonner PLR (1998) Detection of Ca^{2+}-dependent transglutaminase activity in root and leaf tissue of monocotyledonous and dicotyledonous plants. *Plant Physiol.* **117,** 1115-1123.

Mackintosh C (2004) Dynamic interactions between 14-3-3 proteins and phosphoproteins regulate diverse cellular processes. *Biochem. J.* **381,** 329-3242.

Manabe T, Tatsumi K, Inoue M, Matsuyoshi H, Makinodan M, Yokoyama S, Wanaka A (2005) L3/Lhx8 is involved in the determination of cholinergic or GABAergic fate. *J. Neurochem.* **94,** 723-730.

Manecka D-L, Mahmood SF, Grumolato L, Lihrmann I, Anouar Y (2013) Pituitary adenylate cyclase-activating polypeptide (PACAP) promotes both survival and neuritogenesis in PC12 cells through activation of nuclear factor κB (NF-κB) pathway. *J. Biol. Chem.* **288,** 14936-14948.

Manngiavacchi S, Wolf ME (2004) D1 dopamine receptor stimulation increases the rate of AMPA receptor insertion onto the surface of cultured nucleus accumbens neurons through a pathway dependent on protein kinase A. *J Neurochem* **88:** 1261-1271.

May V, Lutz E, Mackenzie C, Schutz KC, Dozark K, Braas KM (2010) Pituitary adenylate cyclase-activating polypeptide (PACAP)/PAC_1HOP1 receptor activation co-ordinates multiple neurotrophic signaling pathways. *J. Biol. Chem.* **285,** 9749-9761.

May V, Clason TA, Buttolph TR, Girard BM, Parsons RL (2014) Calcium influx, but not intracellular calcium release, supports PACAP-mediated ERK activation in HEK PAC1 receptor cells. *J. Mol. Neurosci.* **54,** 342-350.

Mhaouty-Kodja S (2004) Ghα/tissue transglutaminase 2: an emerging G protein in signal transduction. *Biol. Cell.* **96,** 363-367.

Min B, Kwon YC, Choe KM, Chung KC (2015) PINK1 phosphorylates transglutaminase 2 and blocks its proteasomal degradation. *J. Neurosci. Res.* **93,** 722-735.

Mishra S, Murphy LJ (2006) Phosphorylation of transglutaminase 2 by PKA at Ser216 creates 14.3.3 binding sites. *Biochem. Biophys. Res. Commun.* **347,** 1166-1170.

Mishra S, Melino G, Murphy LJ (2007) Transglutaminase 2 kinase activity facilitates protein kinase A-induced phosphorylation of retinoblastoma protein. *J. Biol. Chem*. **282,** 18108-18115.

Miura A, Kambe Y, Inoue K, Tatsukawa H, Kurihara T, Griffin M, Kojima S, Miyata A (2013) Pituitary adenylate cyclase-activating polypeptide Type 1 receptor (*PAC1*) gene is suppressed by transglutaminase 2 activation. *J. Biol. Chem.* **288,** 32720-32730.

Monaghan TK, MacKenzie CJ, Plevin R, Lutz EM (2008) PACAP-38 induces neuronal differentiation of human SH-SY5Y neuroblastoma cells via cAMP-mediated activation of ERK and p38 MAP kinases. *J. Neurochem.* **104,** 74-88.

Montejo-López W, Rivera-Ramírez N, Escamilla-Sánchez J, García-Hernández U, Arias-Montaño JA (2016) Heterologous, PKC-mediated desensitization of human histamine H_3 receptors expressed in CHO-K1 cells. *Neurochem Res* **41:** 2415-2424.

Nurminskaya MV, Belkin AM (2012) Cellular functions of tissue transglutaminase. *Int. Rev. Cell Mol. Biol.* **294,** 1-97.

Perry MJ, Mahoney SA, Haynes LW (1995) Transglutaminase C in cerebellar granule neurons: regulation and localization of substrate cross-linking. *Neuroscience* **65,** 1063-1076.

Pratt EPS, Salyer AE, Guerra ML, Hockerman GH (2016) Ca^{2+} influx through L-type Ca^{2+} channels and Ca^{2+}-induced Ca^{2+} release regulate cAMP accumulation and Epac1-dependent ERK1/2 activation in INS-1 cells. *Mol Cell Endocrinol* **419:** 60-71.

Reglodi D, Kiss P, Lubics A, Tamas A. (2011) Review on the protective effects of PACAP in models of neurodegenerative diseases *in vitro* and *in vivo*. *Curr. Pharm. Des.* **17,** 962-972.

Robberecht P, Gourlet P, De Neef P, Woussen-Colle MC, Vandermeers-Piret MC, Vandermeers A, Christophe J (1992) Structural requirements for the occupancy of pituitary adenylate cyclase activating polypeptide (PACAP) receptors and adenylate cyclase activation in human neuroblastoma NB-OK-1 cell membranes. Discovery of PACAP(6-38) as a potent antagonist. *Eur. J. Biochem.* **207,** 239-246.

Rybchyn MS, Slater M, Conlgrave AD, Mason MS (2011) An Akt-dependent increase in canonical Wnt signaling and a decrease in sclerostin protein levels are involved in strontium ranelate-induced osteogenic effects in human osteoblasts. *J Biol Chem* **286:** 23771-23779.

Schaertl S, Prime M, Wityak J, Dominguez C, Munoz-Sanjuan I, Pacifici RE *et al.* (2010) A profiling platform for the characterization of transglutaminase 2 (TG2) inhibitors. *J. Biomol. Screen.* **15,** 478-487.

Singh US, Pan J, Kao Y-L, Joshi S, Young KL, Baker KM (2003) Tissue transglutaminase mediates activation of RhoA and MAP kinase pathways during retinoic acid-induced neuronal differentiation of SH-SY5Y cells. *J. Biol. Chem.* **278,** 391-399.

Slaughter TF, Achyuthan KE, Lai TS, Greenberg CS (1992) A microtiter plate transglutaminase assay utilizing 5-(biotinamido) pentylamine as substrate. *Anal. Biochem.* **205,** 166-171.

Smith PK, Krohn RI, Hermanson GT, Mallia AK, Gartner FH, Provenzano MD *et al. (*1985) Measurement of protein using bicinchoninic acid. *Anal. Biochem.* **150,**76-85.

Stamnaes J, Fleckenstein B, Sollid LM (2008) The propensity for deamidation and transamidation of peptides by transglutaminase 2 is dependent on substrate affinity and reaction conditions. *Biochim. Biophys. Acta* **1784,** 1804-1811.

Stork PJS, Schmitt JM (2002) Crosstalk between cAMP an MAP kinase signalling in the regulation of cell proliferation. *Trends Cell Biol.* **12,** 258-266.

Sutter AP, Maaser K, Gerst B, Krahn A, Zeitz, Scherübl H (2004) Enhancement of peripheral benzodiazepine receptor ligand-induced apoptosis and cell cycle arrest of esophageal cancer cells by simultaneous inhibition of MAPK/ERK kinase. *Biochem Pharmacol* **67:** 1701-1710.

Tremblay RG, Sikorska M, Sandhu JK, Lanthier P, Riecco-Lutkiewiz M, Bani-Yaghoub M (2010) Differentiation of mouse neuro 2A cells into dopamine neurons. *J. Neurosci. Methods.* **186,** 60-67.

Tucholski J, Johnson GVW (2003) Tissue transglutaminase directly regulates adenylyl cyclase resulting in enhanced cAMP-response element-binding protein (CREB) activation. *J. Biol. Chem.* **278,** 26838-26843.

Tucholski J, Lesort M, Johnson GVW (2001) Tissue transglutaminase is essential for neurite outgrowth in human neuroblastoma SH-SY5Ycells. *Neuroscience* **102,** 481-491.

Trigwell SM, Lynch PT, Griffin M, Hargreaves AJ, Bonner PL (2004) An improved colorimetric assay for the measurement of transglutaminase (type II)-(γ-glutamyl) lysine cross-linking activity. *Anal. Biochem.* **330,** 164-166.

Vallejo I, Vallejo M (2002) Pituitary adenylate cyclase-activating polypeptide induces astrocyte differentiation of precursor cells from developing cerebral cortex. *Mol Cell Neurosci* **21:** 671-683.

Vanella L, Raciti G, Barbagallo I, Bonfanti R, Abraham N, Campisi A (2015) Tissue transglutaminase expression during neuronal differentiation of human mesenchymal stem cells. *CNS Neurol. Disord. Drug Targets* **14,** 24-32.

Vaudry D, Falluel-Morel A, Bourgault S, Basille M, Burel D, Wurtz O, Fournier A, Chow BKC, Hashimoto H, Galas L, Vaudry H (2009) Pituitary adenylate cyclase-activating polypeptide and its receptors: 20 years after the discovery. *Pharmacol. Rev.* **61,** 283-357.

Vyas FS, Hargreaves AJ, Bonner PLR, Boocock DJ, Coveney C, Dickenson JM (2016) A_1 adenosine receptor-induced phosphorylation and modulation of transglutaminase 2 activity in H9c2 cells: a role in cell survival. *Biochem. Pharmacol.* **107,** 41-58.

Walther DJ, Peter J-U, Winter S, Höltje M, Paulmann N, Grohmann M *et al*. (2003) Serotonylation of small GTPases is a signal transduction pathway that triggers platelet α-granule release. Cell **115,** 851-862.

Wang H, Chen Y, Zhu H, Wang S, Zhang X, Xu D, Cao K, Zou J (2012) Increased response to β_2-adrenoreceptor stimulation augments inhibition of Ikr in heart failure ventricular myocytes. *PLoS One* **8:** e46186.

Werner K, Neumann D, Seifert R (2014) Analysis of the histamine H_2-receptor in human monocytes. *Biochem Pharmacol* **92:** 369-379.

Zhang J, Lesort M, Guttmann RP, Johnson GVW (1998) Modulation of the *in situ* activity of tissue transglutaminase by calcium and GTP. *J. Biol. Chem.* **273,** 2288-2295.

Figure 1

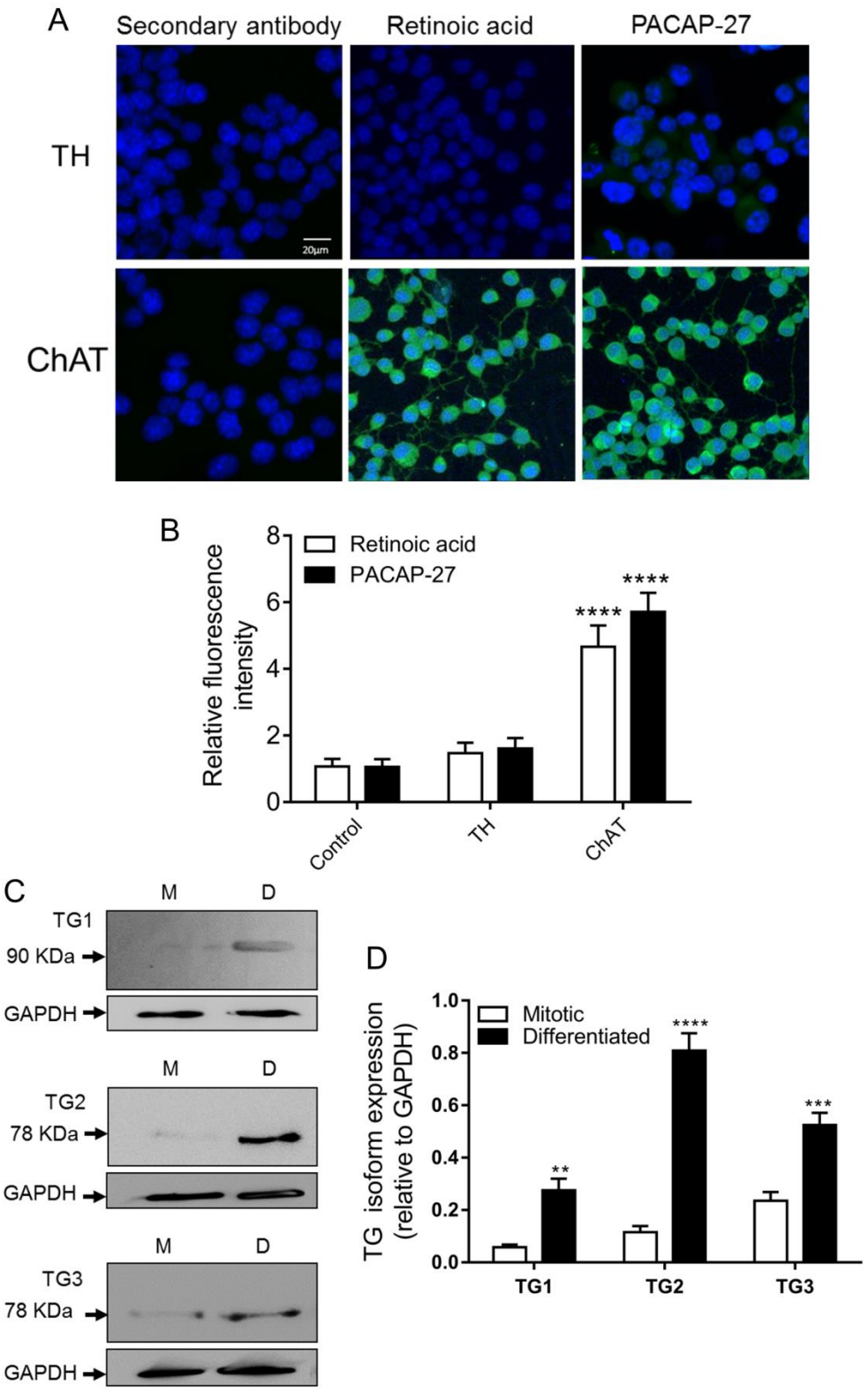
A
Secondary antibody
Retinoic acid
PACAP-27
TH
ChAT
20μm
B
Relative fluorescence intensity
Retinoic acid
PACAP-27
****
****
Control
TH
ChAT
C
M
D
TG1
90 KDa
GAPDH
TG2
78 KDa
GAPDH
TG3
78 KDa
GAPDH
D
TG isoform expression (relative to GAPDH)
Mitotic
Differentiated
**
****
***
TG1
TG2
TG3

Figure 2

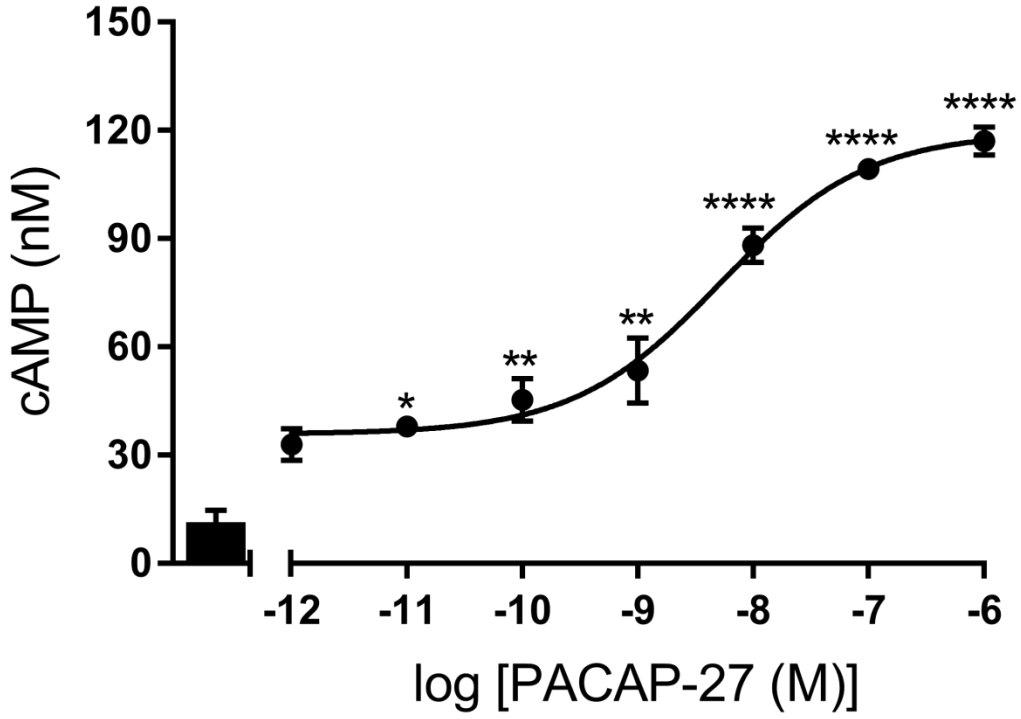

Figure 3

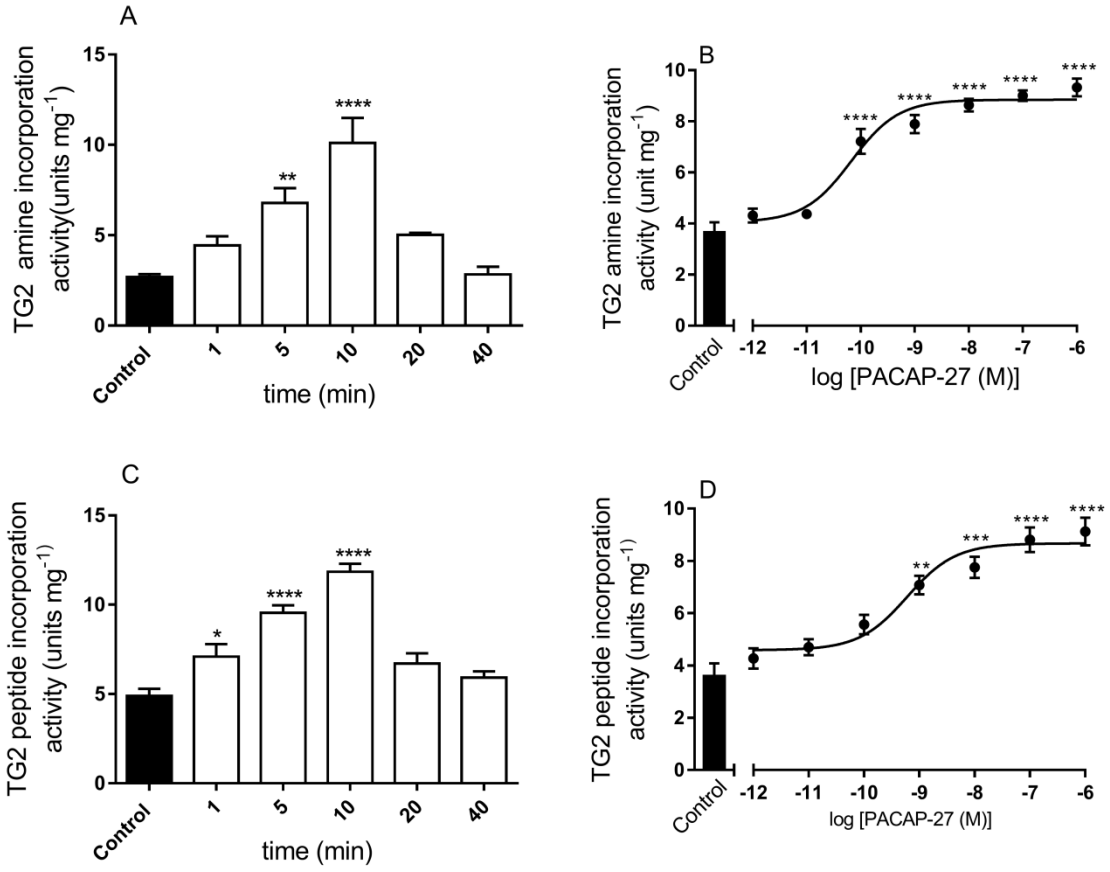
A
TG2 amine incorporation activity(units mg-1)
15
10
5
0
**
****
Control
1
5
10
20
40
time (min)
B
TG2 amine incorporation activity (unit mg-1)
10
8
6
4
2
0
****
****
****
****
****
Control
-12
-11
-10
-9
-8
-7
-6
log [PACAP-27 (M)]
C
TG2 peptide incorporation activity (units mg-1)
15
10
5
0
*
****
****
Control
1
5
10
20
40
time (min)
D
TG2 peptide incorporation activity (units mg-1)
10
8
6
4
2
0
**
***
****
****
Control
-12
-11
-10
-9
-8
-7
-6
log [PACAP-27 (M)]

Figure 4

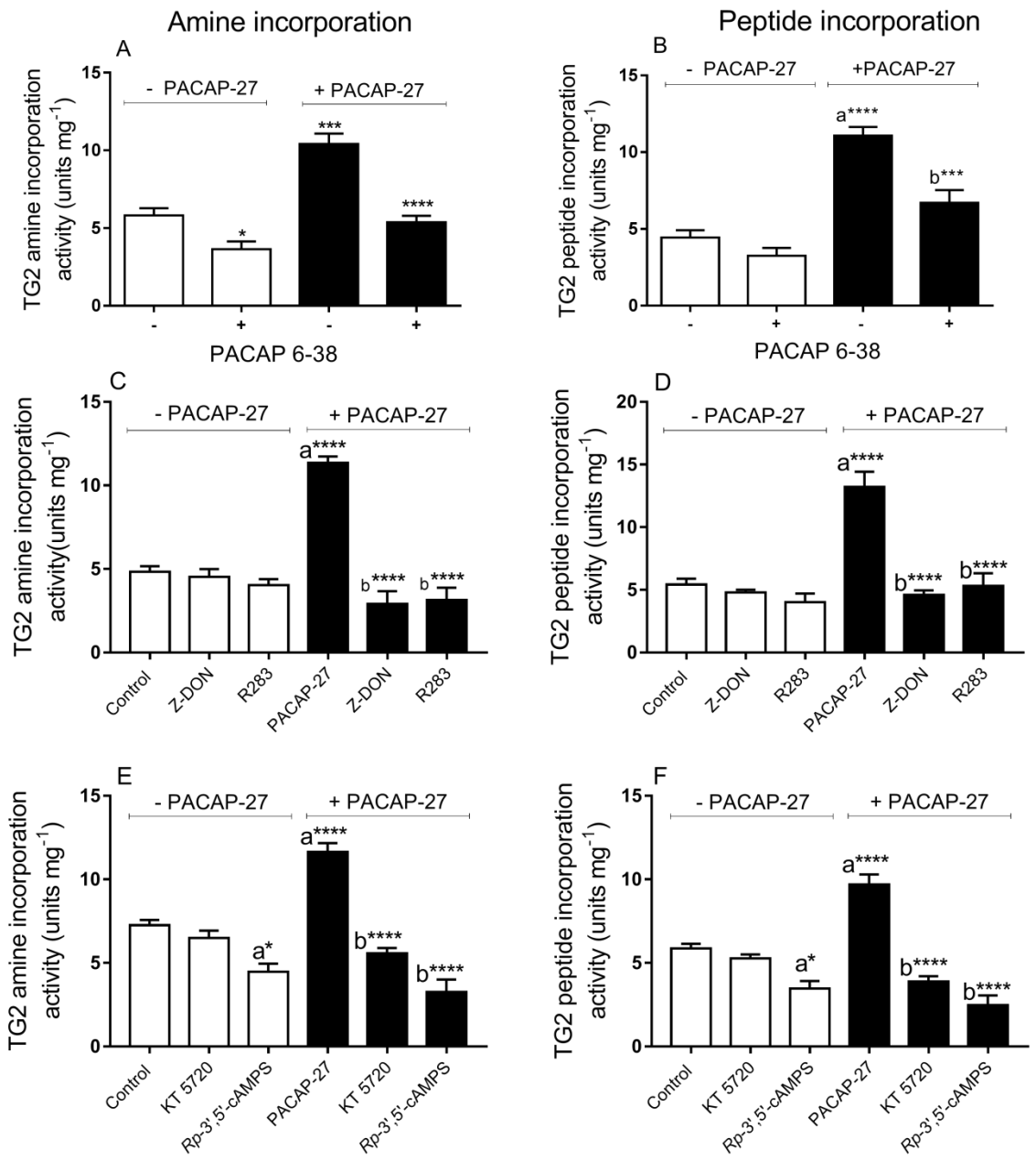
Amine incorporation
Peptide incorporation
A
B
C
D
E
F
- PACAP-27
+ PACAP-27
+PACAP-27
TG2 amine incorporation activity (units mg-1)
TG2 peptide incorporation activity (units mg-1)
TG2 amine incorporation activity(units mg-1)
PACAP 6-38
Control
Z-DON
R283
PACAP-27
KT 5720
Rp-3',5'-cAMPS

Figure 5

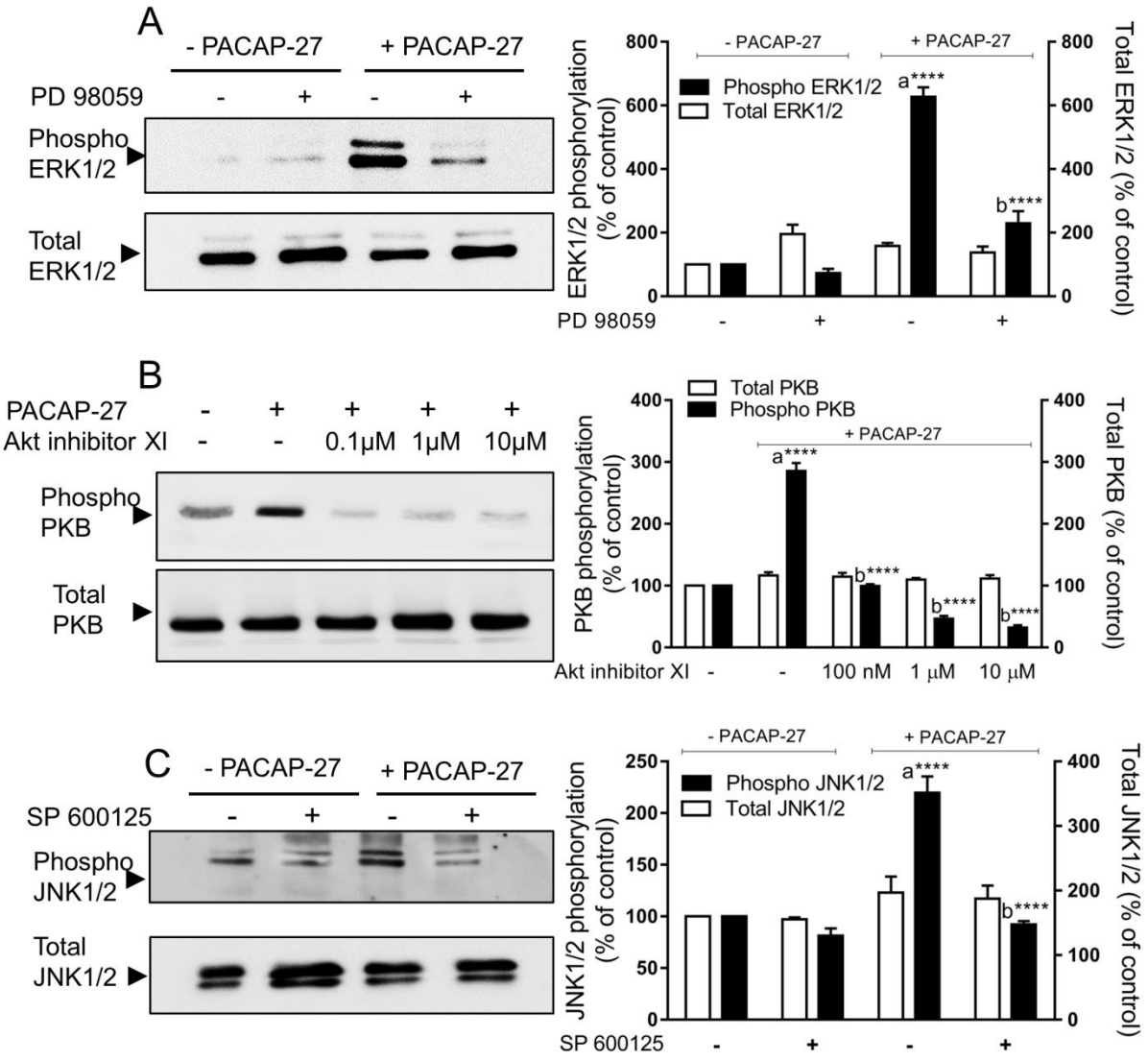
A
- PACAP-27
+ PACAP-27
PD 98059
Phospho ERK1/2
Total ERK1/2
Phospho ERK1/2
Total ERK1/2
ERK1/2 phosphorylation (% of control)
Total ERK1/2 (% of control)
a****
b****
B
PACAP-27
Akt inhibitor XI
0.1μM
1μM
10μM
Phospho PKB
Total PKB
Total PKB
Phospho PKB
PKB phosphorylation (% of control)
Total PKB (% of control)
100 nM
1 μM
10 μM
C
SP 600125
Phospho JNK1/2
Total JNK1/2
Phospho JNK1/2
Total JNK1/2
JNK1/2 phosphorylation (% of control)
Total JNK1/2 (% of control)

Figure 6

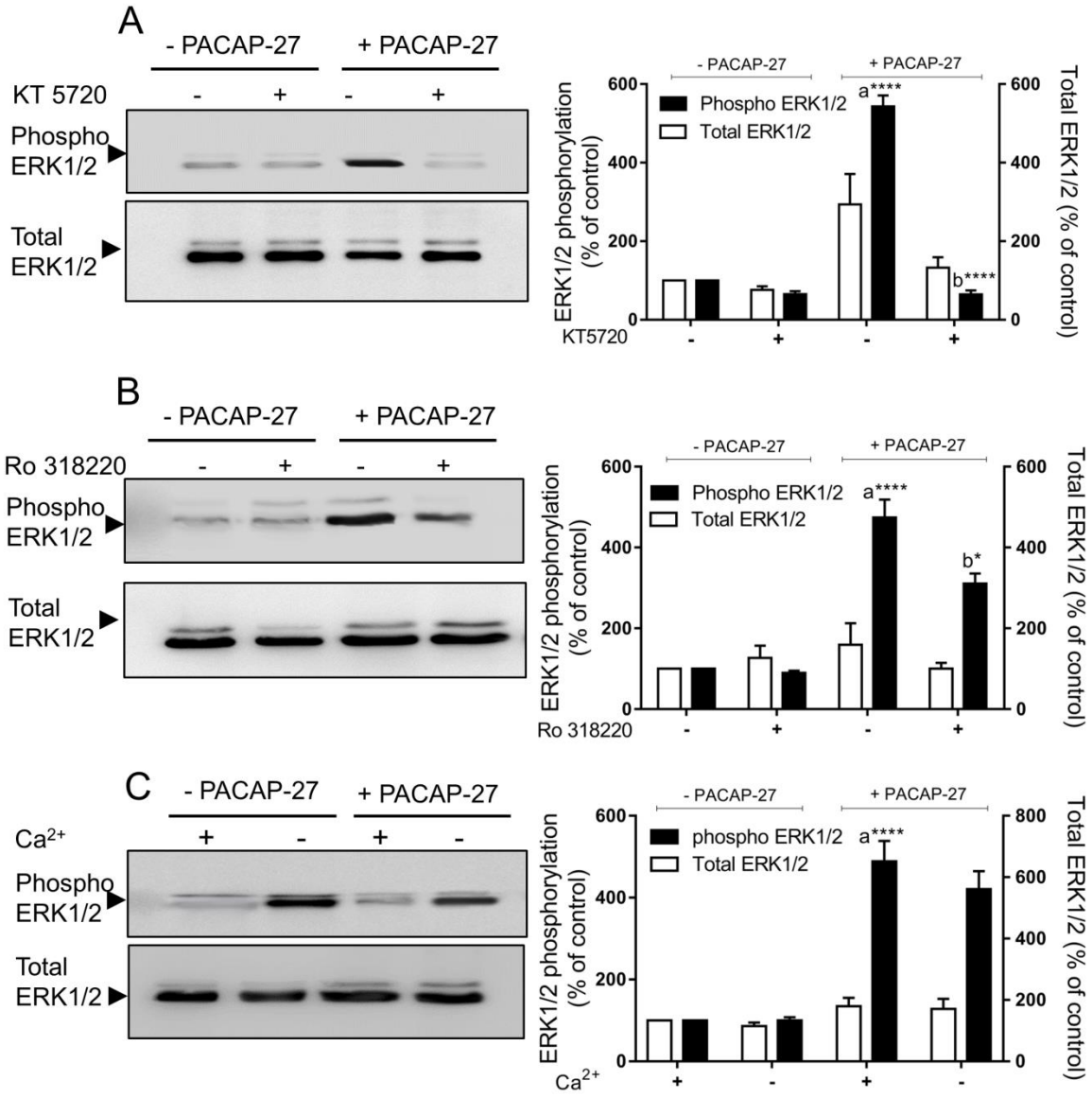
A
- PACAP-27
+ PACAP-27
KT 5720
Phospho ERK1/2
Total ERK1/2
Phospho ERK1/2
Total ERK1/2
a****
b****
ERK1/2 phosphorylation (% of control)
Total ERK1/2 (% of control)
KT5720
B
Ro 318220
a****
b*
Ro 318220
C
Ca2+
phospho ERK1/2
a****
Ca2+

Figure 7

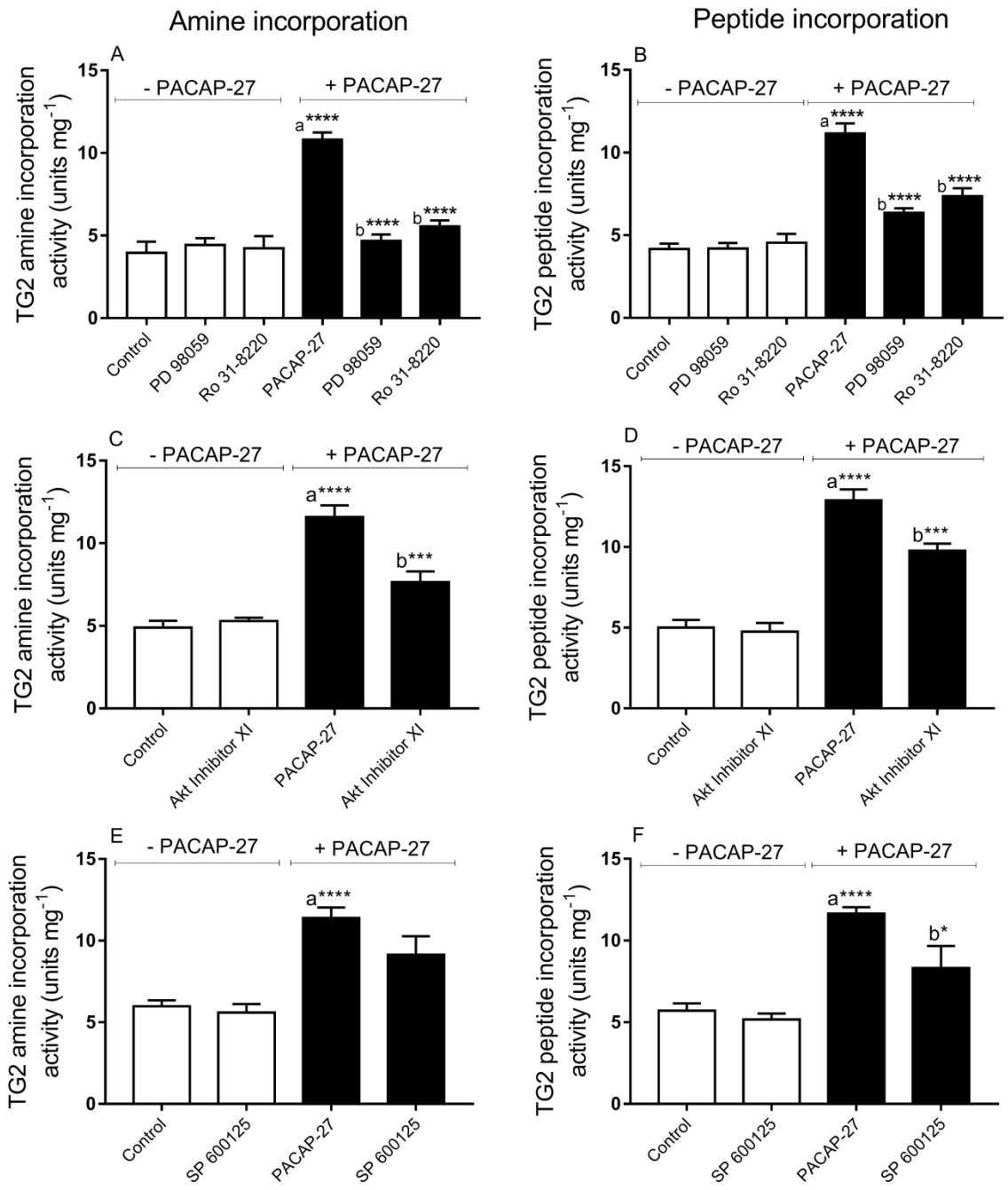
Amine incorporation
Peptide incorporation
A
B
C
D
E
F
- PACAP-27
+ PACAP-27
TG2 amine incorporation activity (units mg-1)
TG2 peptide incorporation activity (units mg-1)
a****
b****
b***
b*
Control
PD 98059
Ro 31-8220
PACAP-27
Akt Inhibitor XI
SP 600125

Figure 8

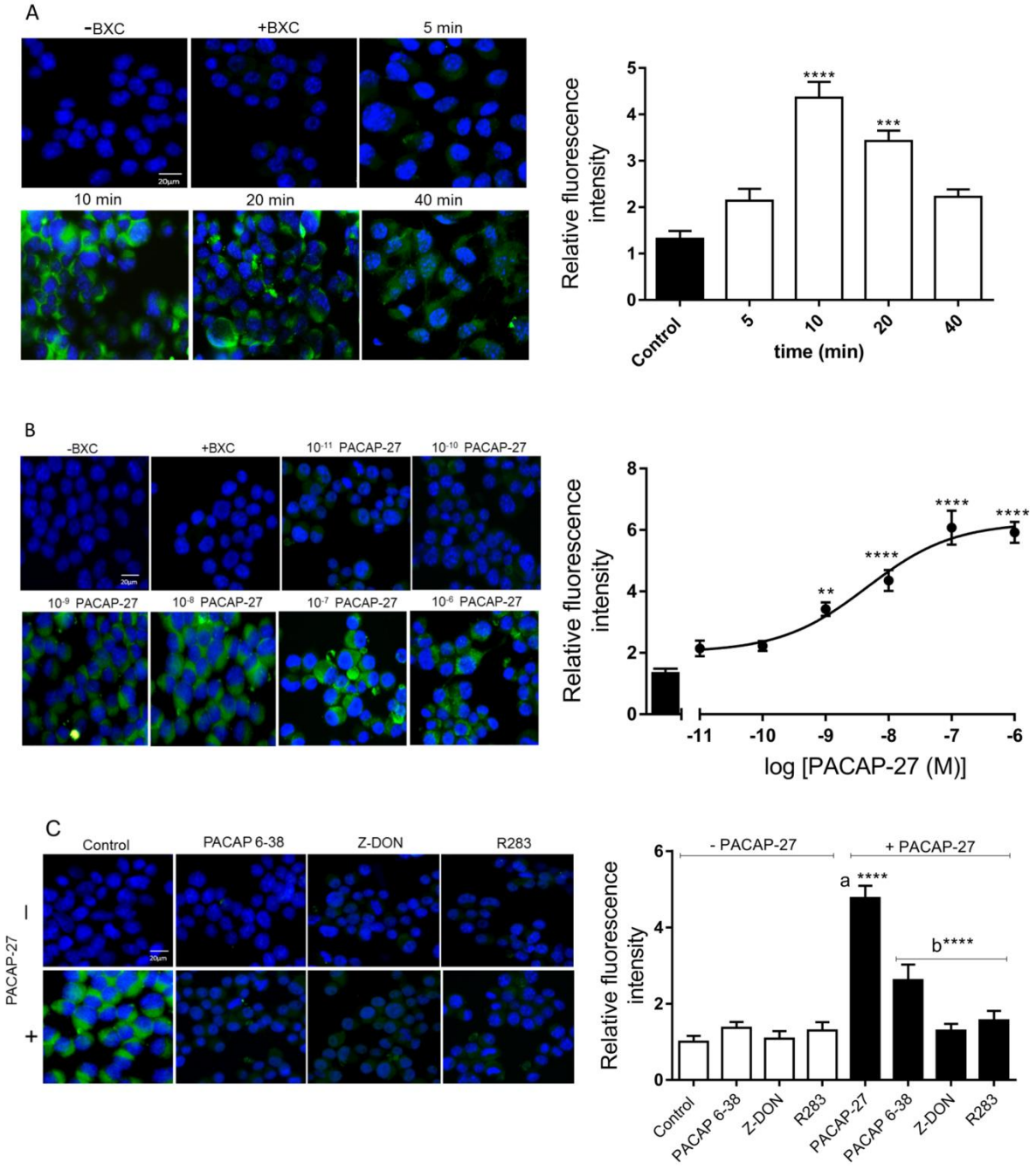
A
-BXC
+BXC
5 min
10 min
20 min
40 min
20µm
Relative fluorescence intensity
****
***
Control
5
10
20
40
time (min)
B
-BXC
+BXC
10-11 PACAP-27
10-10 PACAP-27
10-9 PACAP-27
10-8 PACAP-27
10-7 PACAP-27
10-6 PACAP-27
**
log [PACAP-27 (M)]
C
Control
PACAP 6-38
Z-DON
R283
PACAP-27
- PACAP-27
+ PACAP-27
a ****
b****

Figure 9

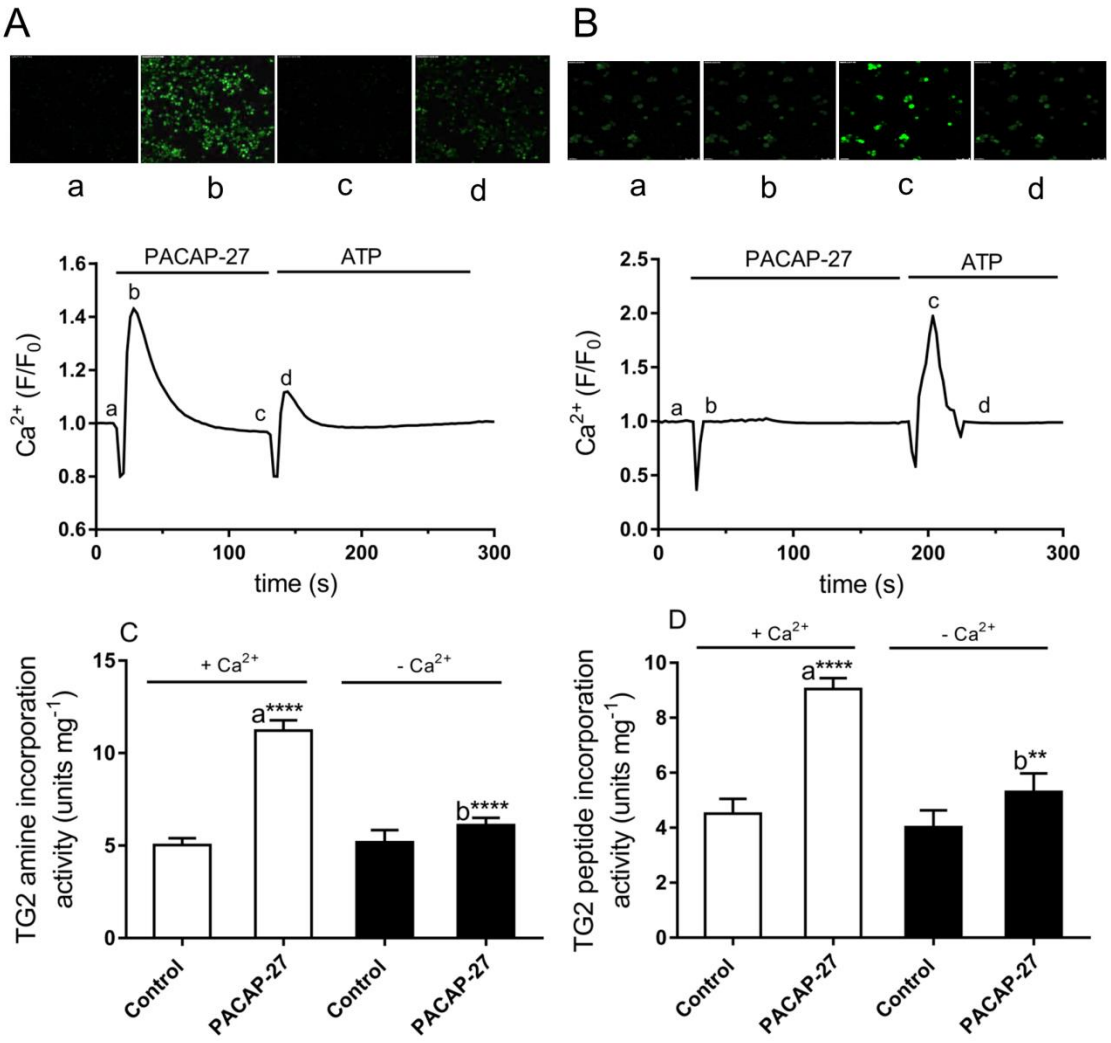
A
B
a
b
c
d
PACAP-27
ATP
Ca2+ (F/F0)
time (s)
C
D
+ Ca2+
- Ca2+
TG2 amine incorporation activity (units mg-1)
TG2 peptide incorporation activity (units mg-1)
a****
b****
b**
Control
PACAP-27

Figure 10

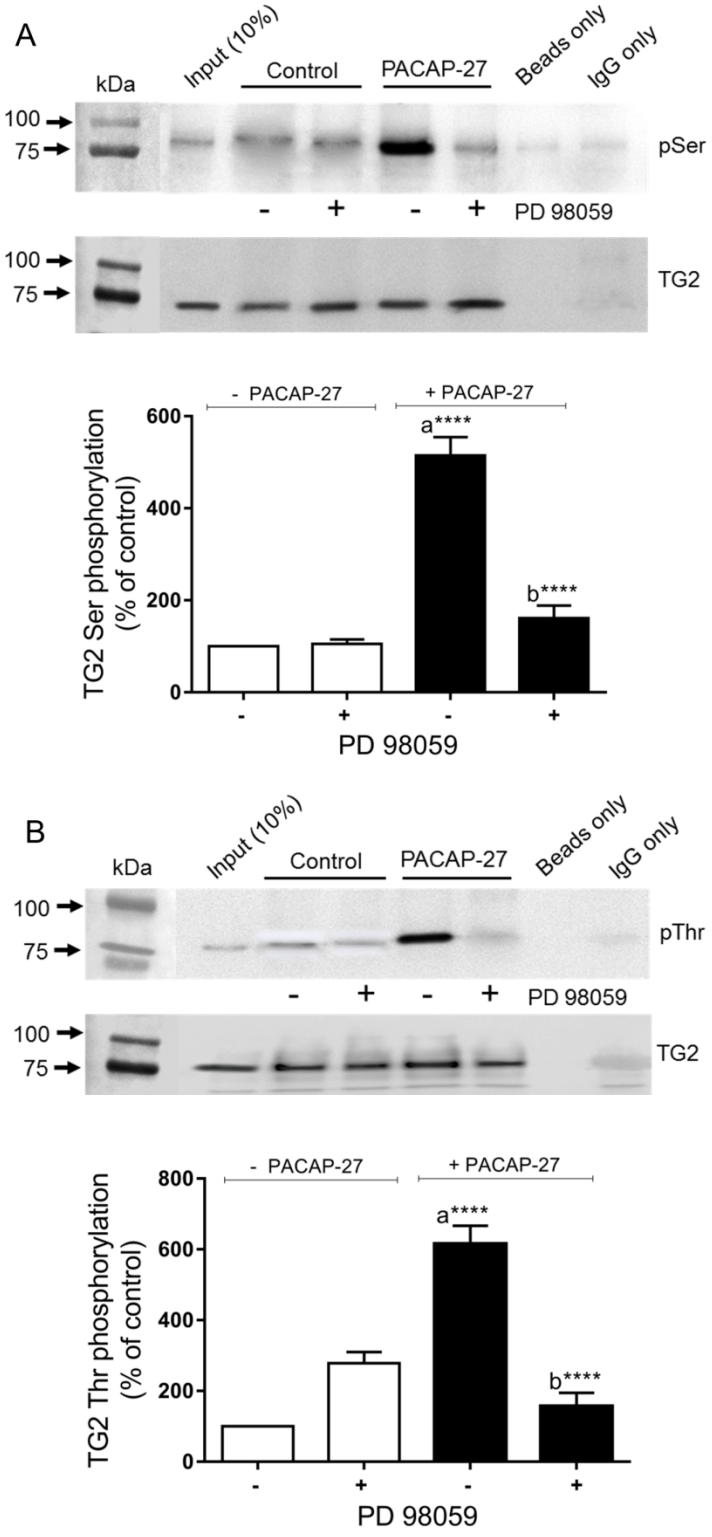
A
kDa
Input (10%)
Control
PACAP-27
Beads only
IgG only
100
75
pSer
- + - + PD 98059
100
75
TG2
- PACAP-27
+ PACAP-27
TG2 Ser phosphorylation (% of control)
600
400
200
0
a****
b****
- + - +
PD 98059
B
kDa
Input (10%)
Control
PACAP-27
Beads only
IgG only
100
75
pThr
- + - + PD 98059
100
75
TG2
- PACAP-27
+ PACAP-27
TG2 Thr phosphorylation (% of control)
800
600
400
200
0
a****
b****
- + - +
PD 98059

Figure 11

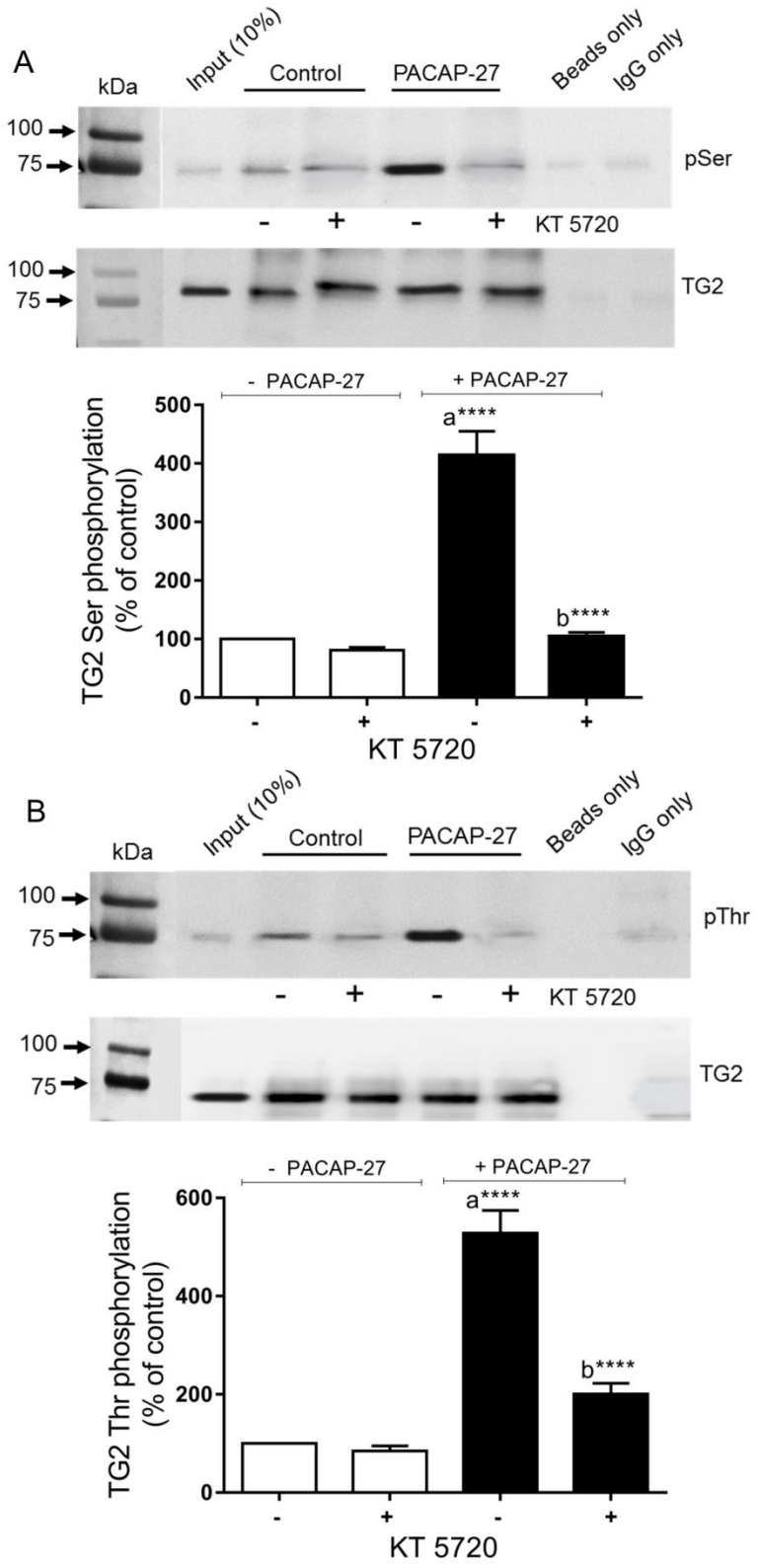
A
kDa
Input (10%)
Control
PACAP-27
Beads only
IgG only
100
75
pSer
- + - + KT 5720
100
75
TG2
- PACAP-27
+ PACAP-27
TG2 Ser phosphorylation (% of control)
500
400
300
200
100
0
a****
b****
- + - +
KT 5720
B
kDa
Input (10%)
Control
PACAP-27
Beads only
IgG only
100
75
pThr
- + - + KT 5720
100
75
TG2
- PACAP-27
+ PACAP-27
TG2 Thr phosphorylation (% of control)
600
400
200
0
a****
b****
- + - +
KT 5720

Figure 12

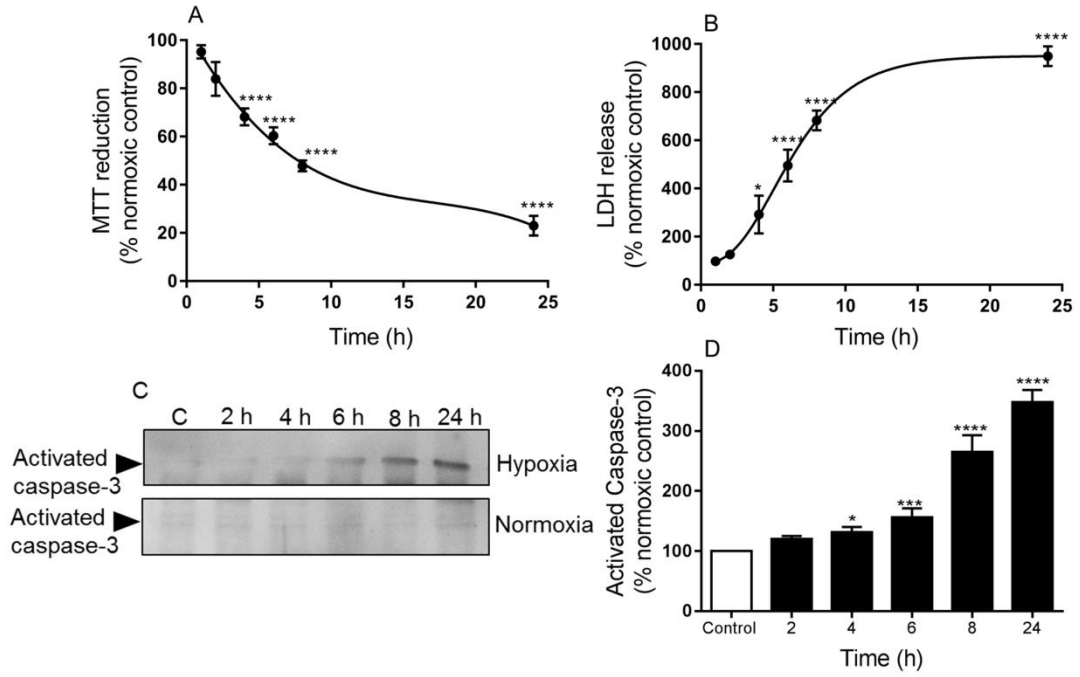
A
MTT reduction (% normoxic control)
Time (h)
B
LDH release (% normoxic control)
Time (h)
C
C 2 h 4 h 6 h 8 h 24 h
Activated caspase-3
Hypoxia
Activated caspase-3
Normoxia
D
Activated Caspase-3 (% normoxic control)
Control 2 4 6 8 24
Time (h)

Figure 13

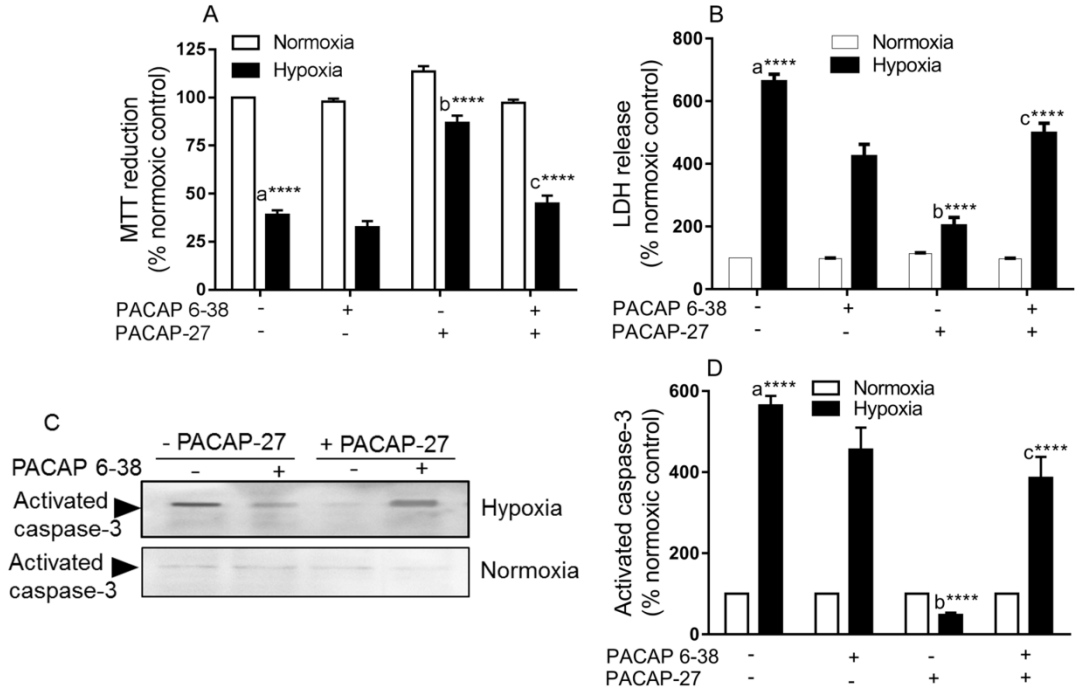
A
Normoxia
Hypoxia
MTT reduction
(% normoxic control)
125
100
75
50
25
0
a****
b****
c****
PACAP 6-38 - + - +
PACAP-27 - - + +
B
Normoxia
Hypoxia
LDH release
(% normoxic control)
800
600
400
200
0
a****
b****
c****
PACAP 6-38 - + - +
PACAP-27 - - + +
C
- PACAP-27
+ PACAP-27
PACAP 6-38
- + - +
Activated
caspase-3
Hypoxia
Activated
caspase-3
Normoxia
D
Normoxia
Hypoxia
Activated caspase-3
(% normoxic control)
600
400
200
0
a****
b****
c****
PACAP 6-38 - + - +
PACAP-27 - - + +

Figure 14

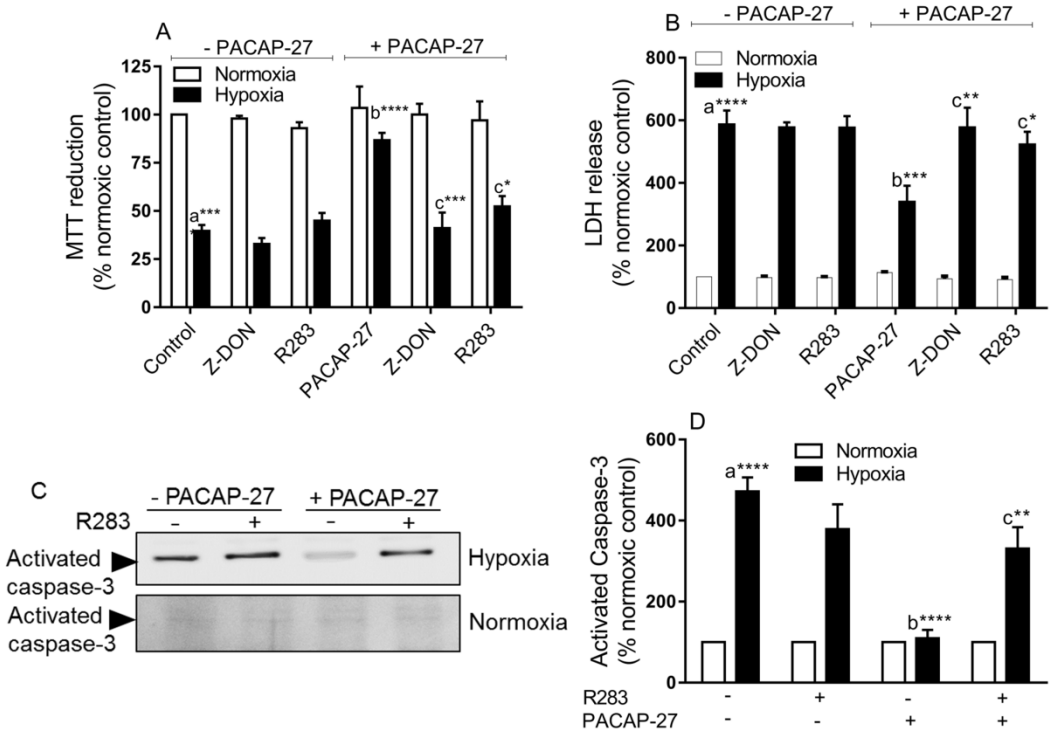
A
- PACAP-27
+ PACAP-27
Normoxia
Hypoxia
MTT reduction
(% normoxic control)
125
100
75
50
25
0
a***
b****
c***
c*
Control
Z-DON
R283
PACAP-27
Z-DON
R283
B
- PACAP-27
+ PACAP-27
Normoxia
Hypoxia
LDH release
(% normoxic control)
800
600
400
200
0
a****
b***
c**
c*
Control
Z-DON
R283
PACAP-27
Z-DON
R283
C
- PACAP-27
+ PACAP-27
R283
-
+
-
+
Activated
caspase-3
Hypoxia
Activated
caspase-3
Normoxia
D
Normoxia
Hypoxia
Activated Caspase-3
(% normoxic control)
600
400
200
0
a****
b****
c**
R283
PACAP-27
-
+
-
+
-
-
+
+

Figure 15

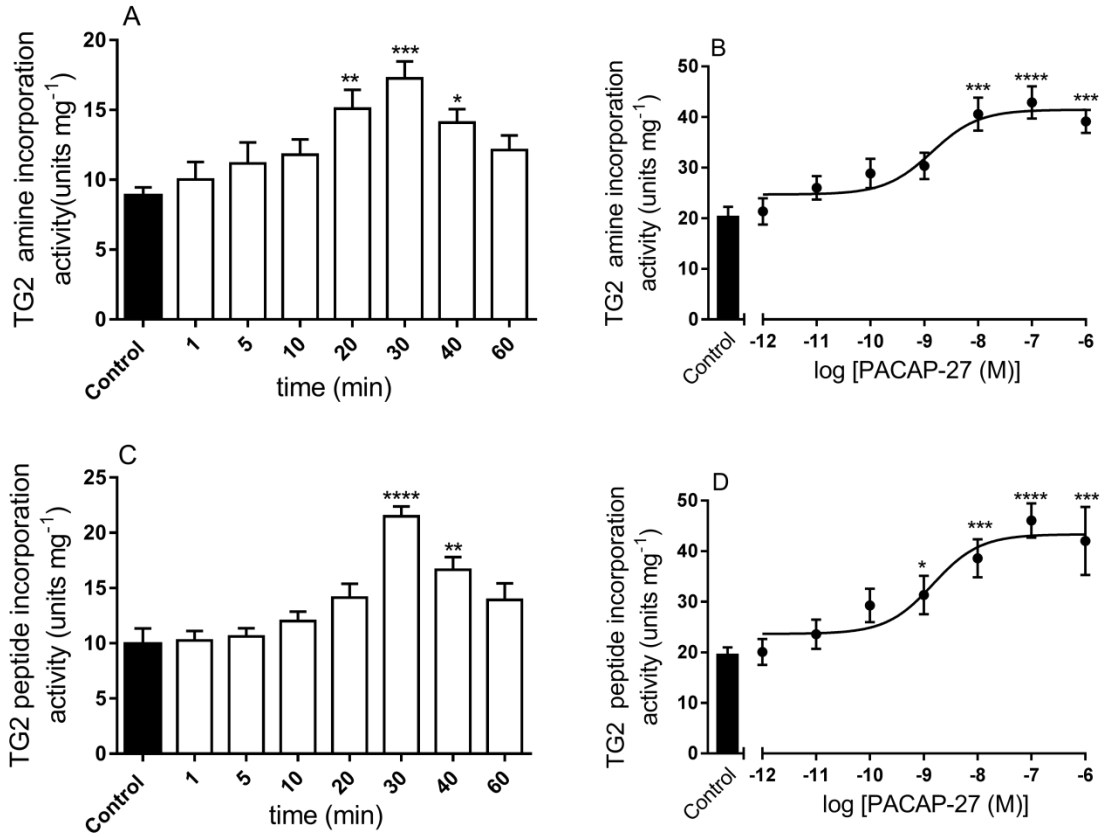
A
TG2 amine incorporation activity(units mg-1)
time (min)
Control
1
5
10
20
30
40
60
B
TG2 amine incorporation activity (units mg-1)
log [PACAP-27 (M)]
C
TG2 peptide incorporation activity (units mg-1)
D
TG2 peptide incorporation activity (units mg-1)

Figure 16 Panels A-D

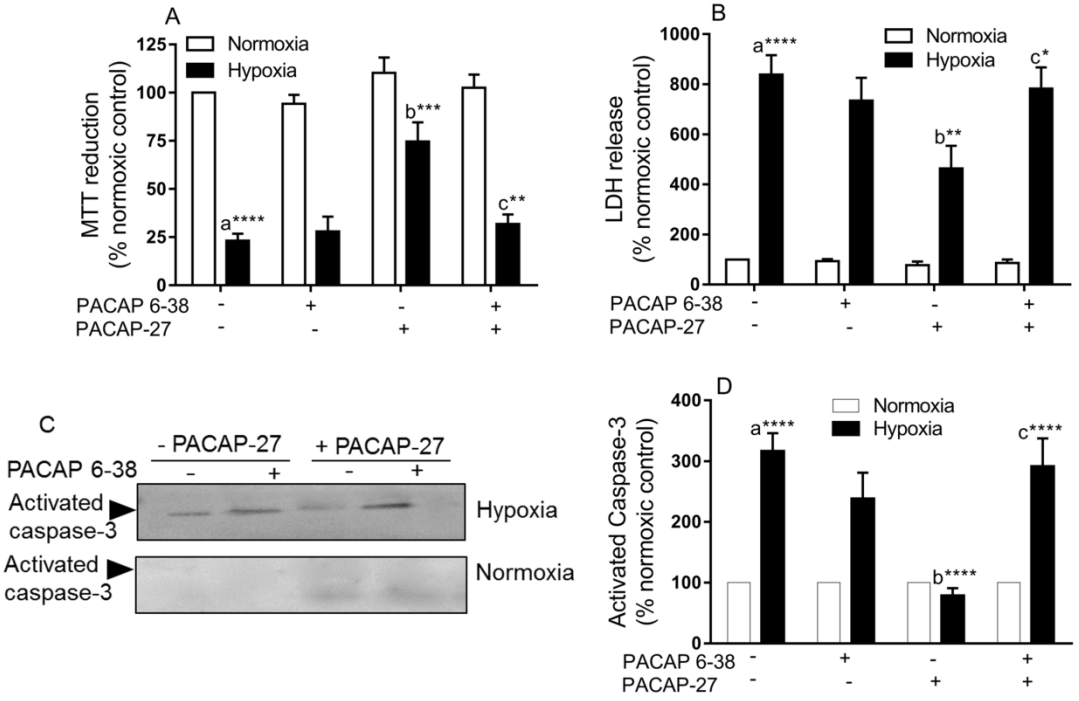

Figure 16 Panels E-H

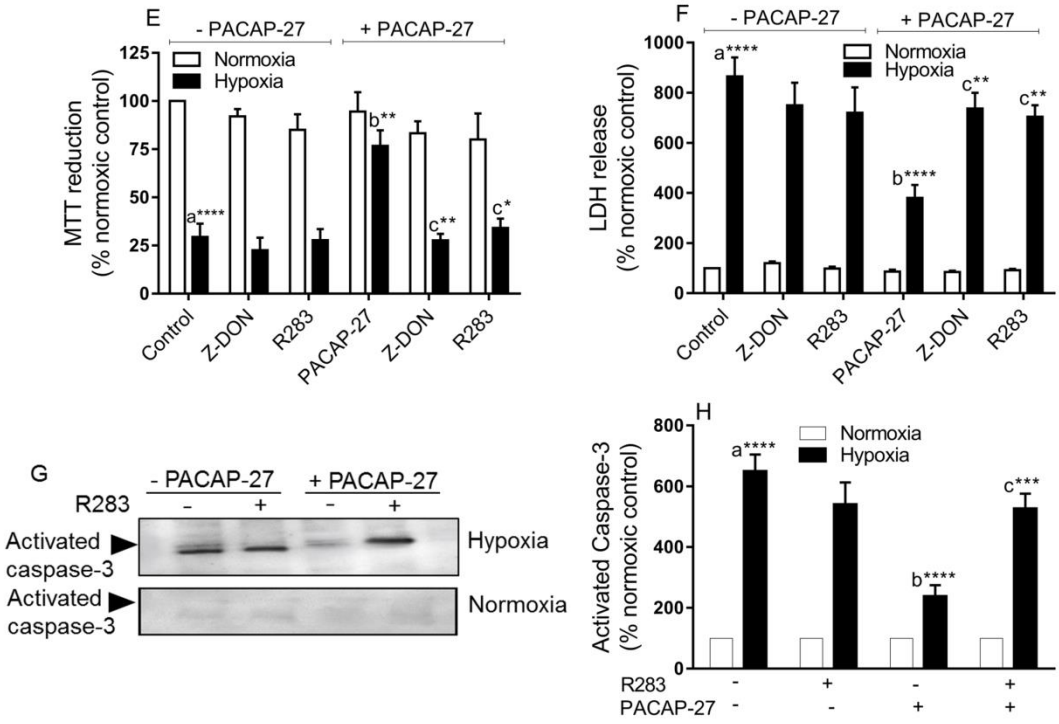

Figure 17

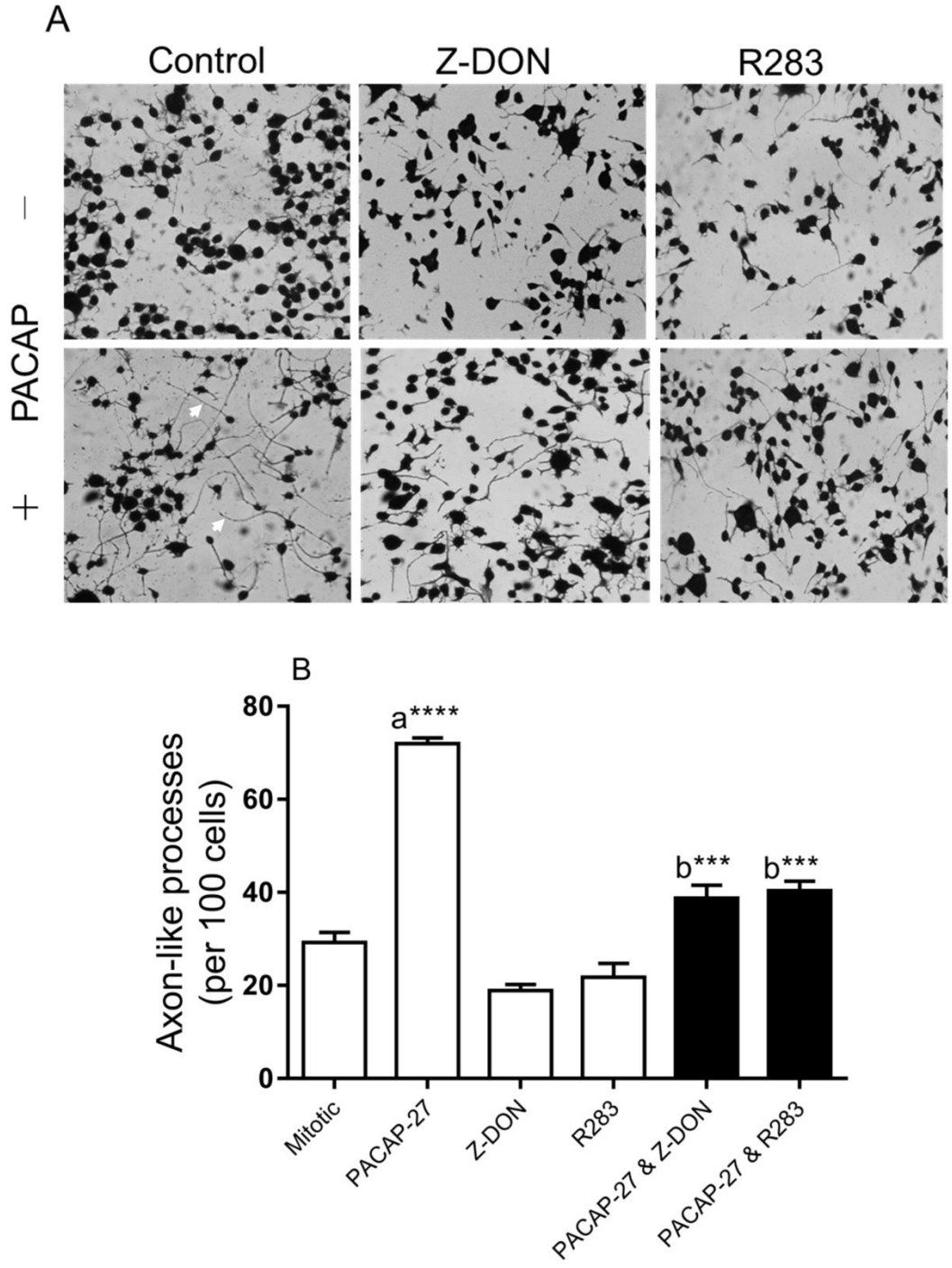
A
Control
Z-DON
R283
PACAP
–
+
B
Axon-like processes
(per 100 cells)
80
60
40
20
0
a****
b***
b***
Mitotic
PACAP-27
Z-DON
R283
PACAP-27 & Z-DON
PACAP-27 & R283